1991-06

An evaluation of the Naval Oceanic Vertical Aerosol Model during Key90

Cecere, Thomas H.

Monterey, California. Naval Postgraduate School

NAVAL POSTGRADUATE SCHOOL
Monterey, California

THESIS

AN EVALUATION OF THE NAVAL OCEANIC VERTICAL AEROSOL MODEL DURING KEY90

by

Thomas H. Cecere

June 1991

Thesis Advisor K.L. Davidson

Unclassified

security classification of this page

REPORT DOCUMENTATION PAGE

a Report Security Classification Unclassified		1b Restrictive Markings	
a Security Classification Authority		3 Distribution Availability of Report	
b Declassification Downgrading Schedule		Approved for public release; distribution is unlimited.	
Performing Organization Report Number(s)		5 Monitoring Organization Report Number(s)	
a Name of Performing Organization Naval Postgraduate School	6b Office Symbol *(if applicable)* 35	7a Name of Monitoring Organization Naval Postgraduate School	
c Address *(city, state, and ZIP code)* Monterey, CA 93943-5000		7b Address *(city, state, and ZIP code)* Monterey, CA 93943-5000	
a Name of Funding Sponsoring Organization	8b Office Symbol *(if applicable)*	9 Procurement Instrument Identification Number	
c Address *(city, state, and ZIP code)*		10 Source of Funding Numbers	
		Program Element No	Project No / Task No / Work Unit Accession No

1 Title *(include security classification)* AN EVALUATION OF THE NAVAL OCEANIC VERTICAL AEROSOL MODEL DURING KEY90

2 Personal Author(s) Thomas H. Cecere

3a Type of Report	13b Time Covered	14 Date of Report *(year, month, day)*	15 Page Count
Master's Thesis	From To	June 1991	63

6 Supplementary Notation The views expressed in this thesis are those of the author and do not reflect the official policy or position of the Department of Defense or the U.S. Government.

17 Cosati Codes			18 Subject Terms *(continue on reverse if necessary and identify by block number)*
Field	Group	Subgroup	Aerosol, Radiative Processes, extinction, NOVAM, KEY90

19 Abstract *(continue on reverse if necessary and identify by block number)*

An experiment was conducted in the Florida Keys from 2 - 19 July 1990 to test the performance of the Naval Oceanic Vertical Aerosol Model (NOVAM) in a weak-convective regime. Meteorological data collected by aircraft and boat was used to generate the surface and vertical profile information files required by NOVAM. Using this information, NOVAM predicts the aerosol extinction (km^{-1}) for a vertical cross-section of the atmosphere. Aircraft-observed aerosol extinction profiles were also obtained. Comparisons between observed and NOVAM aerosol extinction profiles revealed major deviations above the cloud top. From the surface to the top of the cloud layer, NOVAM generally did an excellent job in predicting profile shape, with the magnitude of aerosol extinction tied to the extinction matched at the surface. In a few cases, observed extinction increased more rapidly than NOVAM predicted extinction from the surface to the base of the cloud layer. This is attributed to rain scavenging associated with thunderstorm activity in the area. Comparison between different aerosol extinction profiles revealed much spatial and temporal variation that was verified by Lidar profiles of atmospheric structure. Thunderstorm activity, multiple cloud-layers, and the spatial variation in the atmospheric structure have led to a hypothesis that deep-convection was responsible for the major differences between observed and predicted aerosol extinction profiles. If this is the case, a simple modification to the weak-convective model may be made to apply to a deep-convection model.

20 Distribution Availability of Abstract	21 Abstract Security Classification	
☒ unclassified unlimited ☐ same as report ☐ DTIC users	Unclassified	
22a Name of Responsible Individual T.L. Davidson	22b Telephone *(include Area code)* (408) 646-2309	22c Office Symbol MR(Ds)

DD FORM 1473,84 MAR 83 APR edition may be used until exhausted
All other editions are obsolete

security classification of this page

Unclassified

Approved for public release; distribution is unlimited.

An Evaluation of the Naval Oceanic
Vertical Aerosol Model During Key90

by

Thomas H. Cecere
Lieutenant, United States Navy
B.S., State University of New York at Stony Brook, 1982

Submitted in partial fulfillment of the
requirements for the degree of

MASTER OF SCIENCE IN METEOROLOGY AND PHYSICAL OCEANOGRAPHY

from the

NAVAL POSTGRADUATE SCHOOL
June 1991

Robert L. Haney, Chairman,
Department of Meteorology

ABSTRACT

An experiment was conducted in the Florida Keys from 2 - 19 July 1990 to test the performance of the Naval Oceanic Vertical Aerosol Model (NOVAM) in a weak-convective regime. Meteorological data collected by aircraft and boat was used to generate the surface and vertical profile information files required by NOVAM. Using this information, NOVAM predicts the aerosol extinction (km^{-1}) for a vertical cross-section of the atmosphere. Aircraft-observed aerosol extinction profiles were also obtained. Comparisons between observed and NOVAM aerosol extinction profiles revealed major deviations above the cloud top. From the surface to the top of the cloud layer, NOVAM generally did an excellent job in predicting profile shape, with the magnitude of aerosol extinction tied to the extinction matched at the surface. In a few cases, observed extinction increased more rapidly than NOVAM predicted extinction from the surface to the base of the cloud layer. This is attributed to rain scavenging associated with thunderstorm activity in the area. Comparison between different aerosol extinction profiles revealed much spatial and temporal variation that was verified by Lidar profiles of atmospheric structure. Thunderstorm activity, multiple cloud-layers, and the spatial variation in the atmospheric structure have led to a hypothesis that deep-convection was responsible for the major differences between observed and predicted aerosol extinction profiles. If this is the case, a simple modification to the weak-convective model may be made to apply to a deep-convection model.

TABLE OF CONTENTS

LIST OF FIGURES

LIST OF TABLES

ACKNOWLEDGEMENTS

As much as I would like to say I did it all myself, that simply is not the truth. At the top of my list, I must thank Professor Kenneth L. Davidson for providing his brand of eternal optimism, even when this thesis was in its darkest hours. Additionally, inputs from Professor (and fellow Seaslug) Philip A. Durkee and Mathieu Rouault (when he wasn't out surfing!) proved to be invaluable. The most rewarding experience for me was meeting and working with the scientists involved in the KEY90 experiment. Special thanks to Stu Gathman and Gerrit de Leeuw for their personal contributions, in addition to the numerous references they provided. Obviously, without data provided by the KEY90 team, there wouldn't be many results to talk about, therefore I greatly appreciate the efforts of Doug Jensen, Bill Hooper, Keith Jones, and the many others involved. Last, but certainly not least, I wish to thank my family and friends that have supported me throughout.

I. INTRODUCTION

Successful employment of modern weapon systems require the continuous ability to use wavelengths in the electro-magnetic (EM) spectrum. This is the fundamental concept of electronic warfare and such importance has been placed on this mission area that the following maxim was developed; 'The side that controls the electro-magnetic (EM) spectrum controls the outcome of any conflict in modern war or global politics'. Operation Desert Storm was successful for many reasons, one of which was the allied forces superiority in the maintained use of systems operating at various wavelengths throughout the EM spectrum. Even with this superiority, there is much room for improvement. One example is the limitation that cloud cover had on operations. Another is operating in regions with extensive aerosol content (such as were caused by the intentional burning of oil rigs).

Many military devices operate in the visible to the far infrared (IR) wavelengths. Some examples are forward-looking infrared (FLIR), precision guided munitions and other electro-optical (EO) systems. For this reason, there is a great deal of interest in reliable estimation of EO instrumentation performance for vertical and slant-path observations. For systems such as those above, this requires knowledge of the vertical variation of aerosol scattering and absorption in the wavelengths of operation.

LOWTRAN 7 (Low resolution transmittance model version 7) calculates atmospheric scattering and absorption caused by aerosols and molecules along a non-homogeneous path. Because there isn't one aerosol model that predicts scattering and absorption the best under all conditions, there are different aerosol models a user of LOWTRAN may choose. For maritime applications, the present model is the Navy Aerosol Model (NAM). NAM attempts to relate aerosol size distributions to meteorological parameters such as relative humidity, wind speed, and visibility, and then calculate the optical properties of the modeled aerosol. Most empirical models, such as NAM, do not predict the vertical distribution of aerosol required to extend extinction predictions to higher levels. For the maritime regime, this led to the development of the Naval Oceanic Vertical Aerosol Model (NOVAM).

The purpose of NOVAM (Gathman, 1989) is to determine the vertical distribution of the aerosol size spectra in the marine environment, used to obtain the associated optical and infrared properties along slant paths within the marine boundary layer. The

means used to achieve this goal are to integrate various marine aerosol studies of a diverse nature into a single model. This integration has led to the development of submodels within NOVAM, one of which is selected based on the parameters that are input.

This thesis will investigate the performance of NOVAM under conditions of weak cumulus convection. These conditions existed during the KEY90 experiment which took place from 2 July 1990 through 19 July 1990, near Marathon, Florida on the Florida Keys (Figure 1).

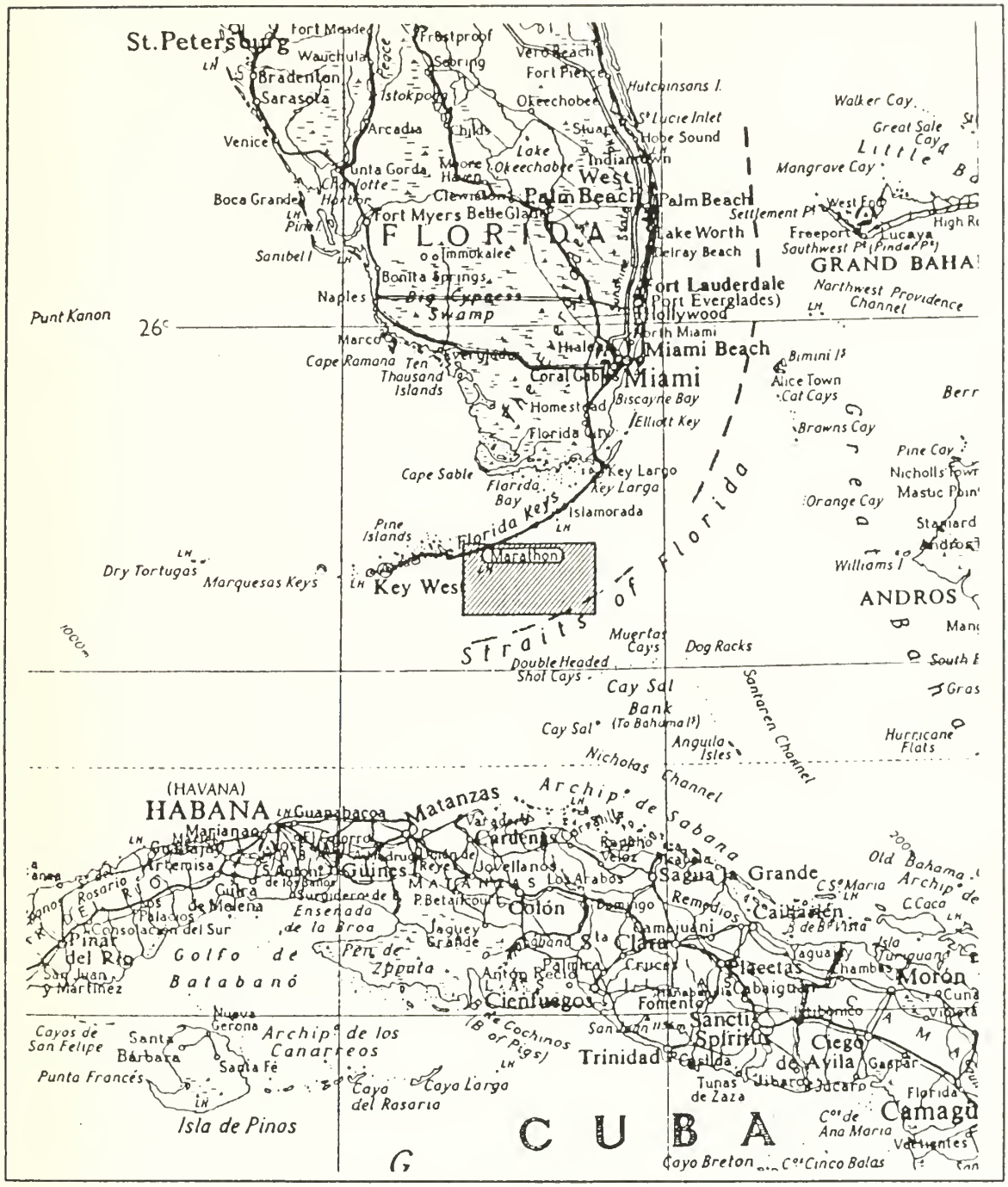

Figure 1. KEY90 experimental area around Marathon (shaded area)

II. BACKGROUND

A. EXTINCTION PARAMETERS

In this section, fundamental concepts and terms that form the basis of the LOWTRAN model, and led to the development of NAM and NOVAM are presented. Lambert, Beer and Bouguet established a relationship between attenuated radiation and the incident radiation for a homogeneous extinction as follows:

$$I = I_o \exp(-bx) \tag{1}$$

where I is the attenuated radiation,

I_o is the incident radiation,

b is the total extinction coefficient,

x is the path length.

To determine the total extinction coefficient, b, knowledge that extinction is caused by absorption and scattering by molecules and aerosol (dry or liquid) contributing linearly is applied as follows:

$$b = b_{ma} + b_{ms} + b_{aa} + b_{as} \tag{2}$$

where b_{ma} = extinction due to molecular absorption,

b_{ms} = extinction due to molecular (Rayleigh) scattering,

b_{aa} = extinction due to aerosol absorption,

b_{as} = extinction due to aerosol (Mie) scattering.

In the visible region of the spectrum, b_{as} and b_{ms} are the dominant extinction components. In the IR regions, b_{ma} and b_{as} are the primary components causing lowered transmittance (the ratio of I to I_o). Figure 2 on page 5 shows the effect molecular absorption has on transmittance over a horizontal 1.82 km path for wavelengths up to 15 μm. This figure clearly demonstrates that atmospheric total extinction is wavelength dependant due to at least its b_{ma} component.

Equation 1 assumes a homogeneous total extinction throughout the atmosphere. Atmospheric studies have shown this assumption to generally be valid for horizontal paths (such as Figure 2), however, a model needed to be developed to predict the vari-

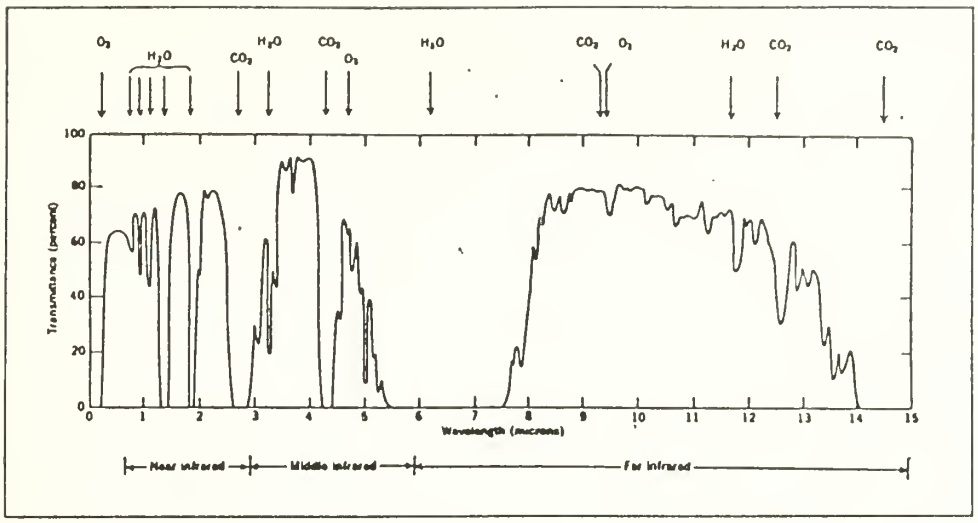

Figure 2. **Atmospheric Transmittance (0 - 15 microns):** Atmospheric Transmittance measured over a 1.82 km horizontal path at sea level (Hudson, 1969).

ations of extinction in the vertical required to perform slant-path calculations. LOWTRAN is the model that resulted from this requirement. LOWTRAN was designed to calculate the total extinction as a function of altitude, and produce as output the radiance and/or the transmittance for a specified path through the atmosphere.

B. THE LOW RESOLUTION TRANSMITTANCE MODEL (LOWTRAN)

LOWTRAN's radiance calculations account for contributions from atmospheric self-emission, solar and/or lunar radiance single scattered into the path, direct solar irradiance through a slant path to space and multiple scattered solar and/or self-emmission radiance into a path. LOWTRAN 7 (the latest version) incorporates separate molecular profiles for all major, as well as 13 minor and trace gases found in the atmosphere. In addition, various aerosol, cloud and rain models are included to allow the user to select the models that most closely represent the region of interest. The user also has the option to select from six reference atmospheric profiles, or define a new atmospheric profile. A more extensive description of LOWTRAN may be found in ONTAR corp. (1990). (Kneizys et al., 1988)

C. THE NAVY AEROSOL MODEL (NAM)

NAM represents one of the several empirically derived models contained in LOWTRAN and was designed to estimate the contribution of aerosol to the EO prop-

agating characteristics in the marine environment. This model predicts an aerosol size distribution (dN/dr) within the atmospheric surface-layer, nominally for 10 meters, for specified wind speed (current and 24-hour averaged), visibility, and relative humidity (RH) values. Three distinct types (modes) of aerosols are assumed to exist within the size distribution:

1. A continental component contributed by a nearby land mass,
2. A stationary component affected by the winds (controlled by the 24-hour averaged wind speed),
3. A fresh component caused by the current wind over the water.

The predicted aerosol size distribution is obtained by summing the contribution of each component as follows:

$$\frac{dN}{dr} = \sum_{r=1}^{3} \frac{A_i}{f_i} \exp\{-[\ln(r) - \ln(f_i - r_{io})]^2\} \tag{3}$$

where N represents the number density per unit radius of particles at radius ,r ,

A_i is the amplitude parameter for mode i,

f_i is the aerosol growth parameter for mode i (to be discussed in a later section),

r_{io} is the mode radius parameter.

When a standard relative humidity of 80% is introduced into the above equation, f_i is replaced by the value one, as will be shown in the relative humidity discussion. A plot of log(dN/dr) at 80% relative humidity versus log(r) is shown in Figure 3. In this figure, A1, A2, and A3 are the amplitude parameters as functions of air mass type, 24-hour averaged wind speed, and current wind speed respectively; and r is the aerosol particle radius at the ambient relative humidity. The mode radius parameter, r_{io}, is the radius that the maximum amplitude parameter value for each mode, i, occurs for this 80% relative humidity. (Gathman, 1983)

NAM's application is to make horizontal path calculations of aerosol extinction at the sea surface based on the following relationship between dN/dr and aerosol extinction (β_{ext}):

$$\beta_{ext} = b_{aa} + b_{as} = \int Q_{ext} \cdot \frac{dN}{dr} \cdot r^2 \cdot dr \tag{4}$$

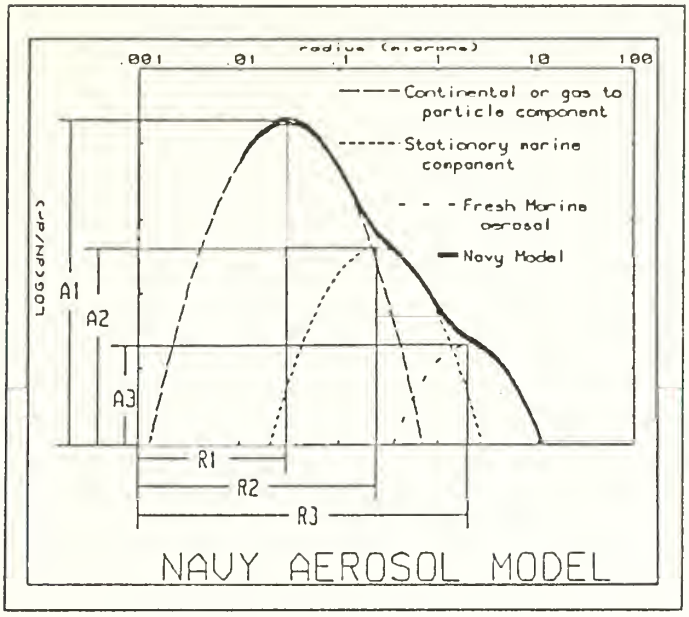

Figure 3. Idealized three lognormal marine aerosol: (Gathman, 1983).

where Q_{ext} is the Mie efficiency coefficient for extinction which is a function of wavelength, causing β_{ext} to be wavelength dependent.

To use NAM in slant path calculations, an assumed vertical size distribution must be developed for each mode based on the size distribution NAM produces at 10 meters. The present assumed size distribution profile has an exponential decrease with height. NOVAM is being developed to provide a capability for more accurate slant-path aerosol extinction calculations in the maritime regime.

D. THE MARITIME ATMOSPHERIC BOUNDARY LAYER (MABL)

Vertical profiles of aerosol depend on the thermodynamic structure and processes within the MABL. A schematic representation of the MABL is shown in Figure 4. In this scheme, the cloud layer varies the most and, at times, may not be present. In cases where the large scale flow prevents cloud development, the MABL terminates at the transition layer. In cases where very deep cloud development has taken place, the top of the MABL is not well defined. Features such as frontogenesis and horizontal advection would cause the one-dimensional view of the MABL (as depicted in Figure 4) to be no longer valid.

For a MABL as shown in Figure 4, the following principles apply: (Augstein, 1976)

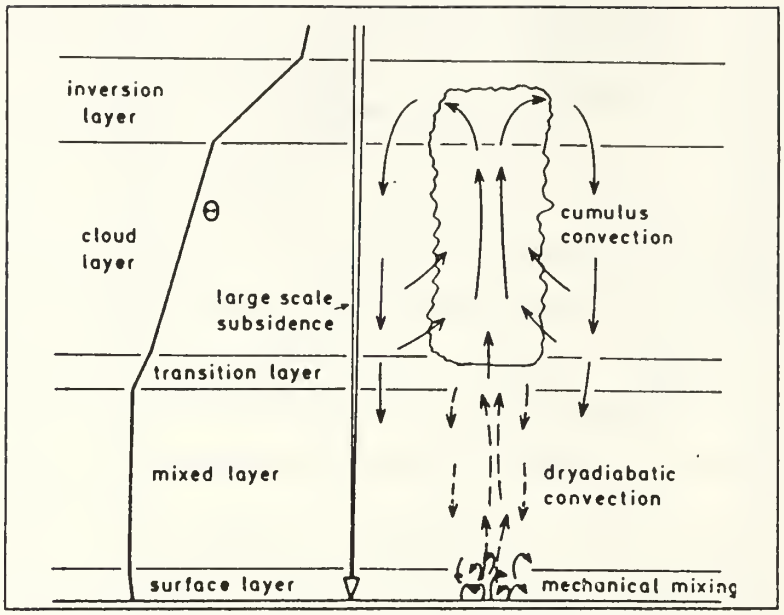

Figure 4. **Schematic of dominant processes in a multi-layered MABL:** θ = potential temperature. (Augstein, 1976)

1. Radiative cooling is compensated for mainly by the adiabatic warming of large-scale subsiding air and, to a lesser extent, by the sensible heat input from the ocean.
2. Buoyancy driven mixing produces a well-mixed region above the shallow surface layer.
3. Kinetic energy which is generated by the concurrent heating and moistening of air from below is partly converted to potential energy through entrainment of potentially warmer air from above through the top of the mixed layer. This assumes that buoyant parcels overshoot their level of equilibrium, thereby forcing mass of less density downward.
4. The top of the mixed layer is determined by a balance of small-scale mass entrainment from below and the large-scale downward mass flow.
5. Clouds begin to develop when convective plumes or bubbles penetrate to their condensation level.

III. THE NAVAL OCEANIC VERTICAL AEROSOL MODEL (NOVAM)

A. BACKGROUND

As described previously, NAM does not predict the correct vertical distributions which are required to extend extinction predictions to higher levels. NOVAM is designed to predict non-uniform and non-logarithmic extinction profiles observed in the MABL for wavelengths between .2 and 40 μm. (Gathman, 1989)

NOVAM is a combination of empirical and physical models which describe aerosol dynamical behavior. The current version of NOVAM incorporates the following models:

1. NAM, which defines the surface (10 meter) aerosol characteristics (Gathman, 1983),
2. Micro-meteorological models, which describe the vertical distribution of aerosol in the well-mixed MABL (Fairall and Davidson, 1986),
3. A model that describes the vertical distribution of aerosol in the weak cumulus convection regime (described below) (Davidson and Fairall, 1986),
4. A model describing the aerosol structure below stratus decks (Noonkester, 1985),
5. A default boundary layer structure model of meteorological parameters based on surface observations (Gathman, 1989),
6. A model that predicts aerosol growth based on relative humidity and the air mass type in the well-mixed and cloud layers (Fitzgerald, 1978; Gerber, 1985).

Extinction properties are calculated from the generated aerosol profiles using MIE scattering for which two basic characteristics exist:

1. The aerosol particle radius and the wavelength of incident energy are of the same order of magnitude.
2. Scattering is generally concentrated in the forward direction (forward scatter).

The following particle source and particle physics principles have been used in the development of NOVAM. Large sea-salt aerosol particles are produced from white water phenomena at the air-sea interface (Monahan et al., 1982). Smaller aerosol particles are produced from sources such as gas-to-particle conversion or anthropologically generated aerosol. The concentration of any particular aerosol is dependant on the source strength of aerosol production and on the mixing process as it relates to scalar contaminants. Regarding hygroscopic sea-salt aerosol, its size is very dependant on the relative humidity it is immersed in. Also, as the hygroscopic aerosol picks up water vapor

from the atmosphere and grows in size, it changes its chemical composition and its index of refraction.

B. NOVAM INPUTS

Tables 1 and 2 show surface and radiosonde observation files (inputs) required by NOVAM. The surface observed parameters are used to perform the size distribution and aerosol extinction calculations at the surface and for sub-model selection, in conjunction with some information contained in Table 2. The cloud type, present weather, and the zonal/seasonal category codes may all be found in separate tables as described by Gathman (1989). If any of these data items are unavailable for input, the model calculates that parameter using default information which results in a reduced confidence in aerosol extinction predictions.

Table 1. SURFACE OBSERVATION DATA FILE

Position	Meteorological Data
1.	Sea surface temperature (°C)
2.	Air temperature (°C)
3.	Relative humidity (RH) (%)
4.	Optical visibility (km)
5.	Current real wind speed (m/s)
6.	Averaged wind speed (24 h) (m/s)
7.	Air mass parameter (see text)
8.	Cloud cover (tenths)
9.	Cloud type [0...9]
10.	Surface IR ext. (1/km) (@ 10.6μm)
11.	Present weather in standard code [0...99]
12.	Height of lowest cloud (m)
13.	Zonal/seasonal category [1...6]

Most of the parameters listed in Table 1 are self explanatory, however, a couple warrant further examination. The air mass parameter is an indicator of the degree of continental contaminants and may be represented as follows:

$$a.m.p. = Rn/4 + 1$$

where Rn represents the atmospheric radon content (picocuries per cubic cm),

Table 2. CONTENTS OF THE RADIOSONDE DATA FILE PREAMBLE

Row	Column	Description
[1][1]	[1]	Number of actual radiosonde observations
[1][1]	[2]	Surface potential temperature from radiosonde
[1][1]	[3]	Surface mixing ratio from radiosonde
		Profile Characteristics
[2]	[1]	Height of base of cloud layer (CB)
[2]	[2]	Potential temperature just below CB
[2]	[3]	Mixing ratio just below CB
[3]	[1]	Units indicator for temperature (= 1 if °C)
[3]	[2]	Potential temperature just above CB
[3]	[3]	Mixing ratio just above CB
[4]	[1]	Height of the cloud layer top (CT)
[4]	[2]	Potential temperature just below CT
[4]	[3]	Mixing ratio just below CT
[5]	[1]	Units indicator for mixing ratio (= 1 if g kg)
[5]	[2]	Potential Temperature just above CT
[5]	[3]	Mixing ratio just above CT

[1] Minimum requirement for radiosonde data file.

or as,

$$a.m.p. = (9 \times \exp[-t/4]) + 1$$

where t equals the elapsed time (in days) it takes the current air mass to reach the point of observation from a distant land mass.

An air mass parameter of 1 indicates a pure air mass (no contaminants). When the air mass parameter is less than or equal to 5, the aerosol is assumed to be made up of three lognormal components (A_1, A_2 , and A_3) as contained in the NAM description above. For air mass parameters greater than 5, indicating the presence of non-soluble aerosol, an additional lognormal component (A_0) is assumed. This class of non-soluble aerosol

is only present close to shore lines and has the same mode radius as r_{1_0} shown in Figure 3. Being assumed non-soluble, the mode 0 component of aerosol does not change size with changes in relative humidity. (Gathman, 1989)

The remaining inputs to NOVAM are contained in a data file describing the vertical atmosphere, referred to as the radiosonde data file in Gathman, 1989. Table 2 shows the format for the first five rows that are contained in this file, necessary when choosing the weak convective model. Figure 5 graphically illustrates the position in the file by row and column designation. The remainder of the radiosonde file consists of radiosonde observation height, potential temperature, and mixing ratio entries. If radiosonde data is not available, a minimum of 1 surface entry must be input and a default profile is selected.

After the input parameters are translated by NOVAM to predictions of mixing, source strengths, and size distributions, a prediction is provided of the extinction of EO energy as a function of altitude for the wavelength of interest. This output is based on the dry aerosol size distribution at a particular height and adjusted for relative humidity at that height.

C. SUB-MODELS

This section is intended to give a brief explanation of the different models being developed within NOVAM. Figure 6 shows the major decision points and the track of flow of information in the current version. There are currently four sub-models in NOVAM:

1. A mixed boundary layer model (Fairall & Davidson, 1986; Davidson & Fairall, 1986) where the boundary layer depth must be less than 3 km and not stable,
2. A stratus model for winds less than 5 m/s model (Noonkester, 1985). Here, the size distribution is not represented by a series of lognormals (as in Figure 3), there is no requirement for calculations to fit NAM predictions at 10 meters, and the wavelengths available for NOVAM calculation are from 1 to 11 μm. The limitation on wavelengths is due to optical calculations using a simplification of Mie scattering parameters.
3. A weak convection model (Davidson & Fairall, 1986) used when scattered cumulus clouds are present, cloud tops do not exceed 3 km, and a well-mixed layer is present below the cloud base,
4. A default profile (Gathman, 1989) which is used when there is no vertical potential temperature and mixing ratio information.

A stratus model for winds greater than 5 m/s and a deep convection model for cloud tops extending above 3000 m are not yet supported.

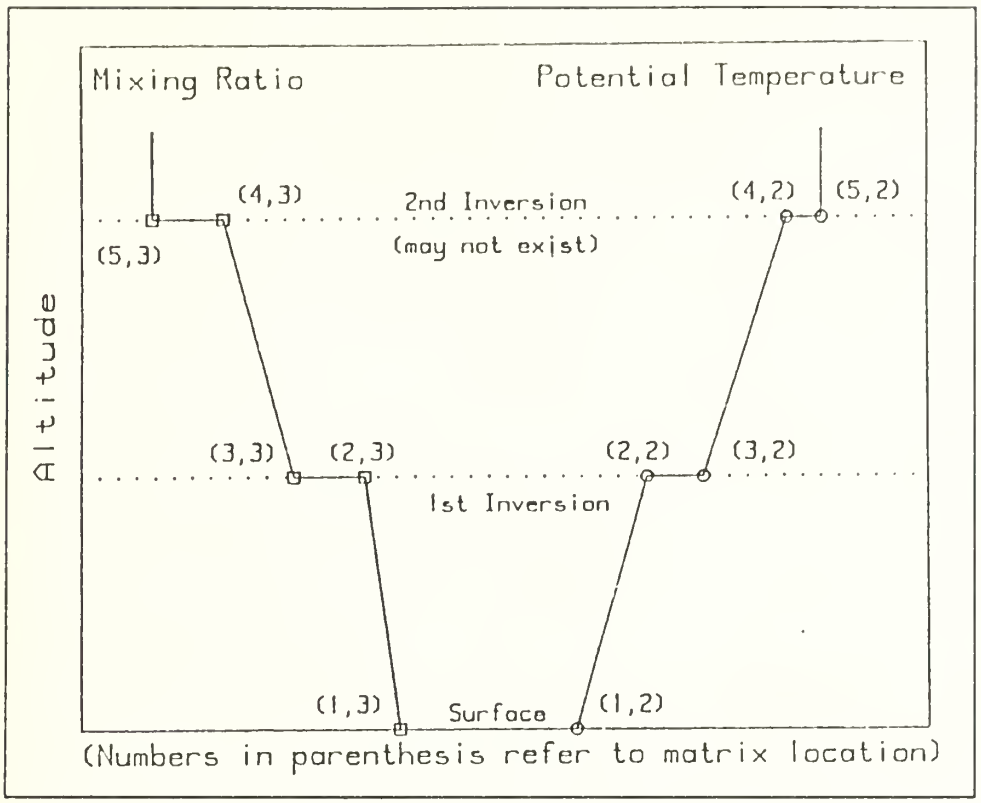

Figure 5. Stylized profile definitions for use in preamble: (Gathman, 1989).

NOVAM sub-model selection is based on the input parameters describing the vertical stratification (thermal stability, presence of an inversion, and the inversion height), cloud cover, cloud type, wind speed, and the requested wavelength for extinction calculations.

1. The default profile generator

The default profile generator uses the surface meteorological measurements to develop profiles of temperature and relative humidity, generating values for every 100 meters of altitude. The default profile differs from a radiosonde derived profile by having the vertical distribution of the lognormal components described by an exponential function of scale height. For each default altitude level, the optical calculations are based on the combined size distributions of the aerosol deduced from the model assumptions. The index of refraction and size are determined by the response (swelling) of hygroscopic aerosols based on the relative humidity calculated from the relative humidity profile

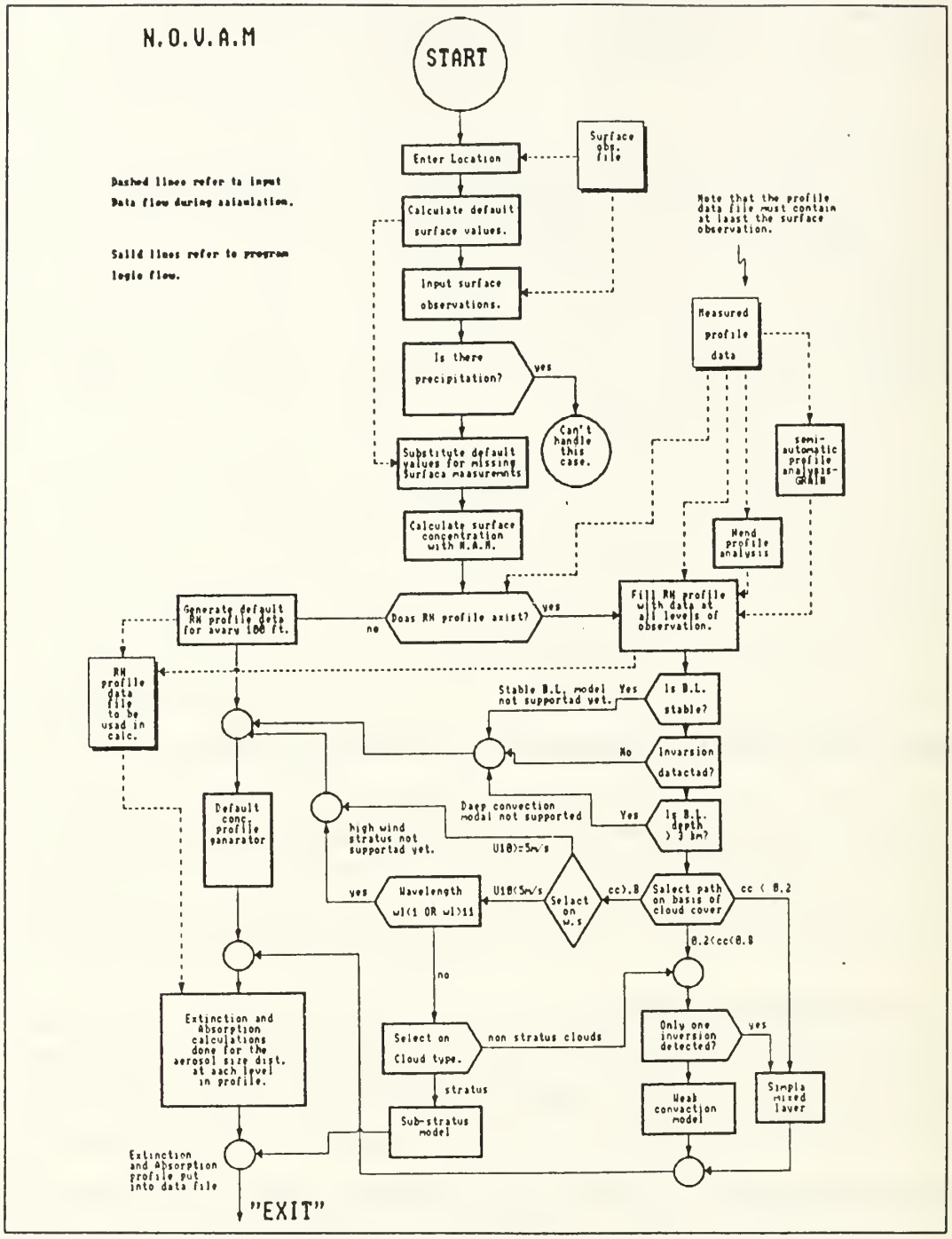

Figure 6. NOVAM flow diagram: (Gathman, 1989).

generator (Gathman, 78). From these parameters, the aerosol extinction at each level can be calculated directly.

IV. INFLUENCES ON AEROSOL SIZE DISTRIBUTION PROFILES WITH WEAK CONVECTION

A. CONCENTRATION GRADIENTS IN NOVAM

The basis for modeling the evolution of aerosol concentration is the continuity equation. In the Boussinesq approximation, which assumes a shallow planetary boundary layer, an incompressible fluid ($\frac{d\rho}{dt} = 0$), and negligible horizontal gradients of density, an aerosol component concentration, X, can be written in its simplest one-dimensional form as

$$\frac{\partial X}{\partial t} + \vec{U}\nabla_H X + W\frac{\partial X}{\partial z} = -\frac{\partial}{\partial z}\left(\overline{WX} - V_g X - D\frac{\partial X}{\partial z}\right) \tag{7}$$

where U is the mean horizontal wind,

W is the mean vertical wind,

V_g is the particle gravitational settling velocity,

D is the particle molecular transport coefficient,

$\overline{WX}$ is the mean vertical flux of particles due to turbulent transport.

In this equation, X must be a conservative aerosol variable, e.g. dry size concentration, that is unaffected by variations in relative humidity. Terms such as $\overline{WX}$ are unlikely to be known from first principles leading to applying models of the boundary layer to simplify the process. (Davidson and Fairall, 1986)

The Albrecht model was developed specifically for a trade-wind region (Albrecht, 1979) and has been incorporated in NOVAM to describe the weak convective regime. The three-layer structure of this regime, described by Albrecht, is shown in Figure 7. In Figure 7, C represents the dry aerosol concentration with the subscripts r, b, c, and i representing the surface, cloud base, the in-cloud layer, and the cloud top respectively. The layers and their characteristics are summarized below, Davidson & Fairall (1986):

1. The subcloud layer ($0 < z < z_b$) where z_b is the cloud base (LCL). This layer is characterized by linear flux profiles and "well-mixed" mean profiles. The depth of this layer is changed by subsidence and entrainment.
2. The cumulus cloud layer ($z_b < z < z_i$), characterized by parabolic flux profiles and linear mean profiles. The slopes of the mean properties are determined by empirical

models of cloud transport and entrainment properties as well as the boundary conditions at the top and bottom of the cloud layer.

3. The free troposphere (non-turbulent) above the capping "trade" inversion. The properties of this layer are determined by advection and are usually input variables to the model.

Note that the mean profiles are not continuous at interfaces z_b and z_i.

Factors that influence the in-cloud dry aerosol concentration gradient, γ (shown in Figure 7), are given by the following balance equation:

$$\frac{D\gamma}{Dt} = (\nabla \cdot \vec{V} - \frac{1}{\tau})\gamma + \frac{E\Delta X_b}{\tau(z_i - z_b)} + \frac{4w'_e \Delta X_i}{(z_i - z_b)^2} \tag{8}$$

where $\nabla \cdot \vec{V}$ is divergence,

w'_e is the entrainment rate of the inversion,

τ is the cloud relaxation time in days,

E is the cloud wall entrainment variable given by:

$$E = \frac{(z_i - z_b)\gamma_e + 2\Delta T_o(1 + \Gamma)}{\Delta\theta_{eb}} \tag{9}$$

where ΔT_o = .5°K,

$\Gamma \simeq 1.6$,

γ_e = the entrainment rate of θ_e in the layer,

$\Delta\theta_{eb}$ is the jump in θ_e at the cloud base.

Because the layer below the cloud base is considered well-mixed, the dry aerosol concentration gradient for this layer is normally considered to be 0, but a non-zero gradient could be predicted by the model with the specified parameters. (Davidson and Fairall, 1986)

Some assumptions were made to simplify calculations when incorporating the Albrecht model into NOVAM. The Albrecht model is dynamic, predicting the temporal evolution of the boundary layer. NOVAM seeks to characterize the average or typical vertical structure, therefore all time derivatives are neglected in the above equations. Additionally, the following assumptions are used to simplify calculations: (Davidson & Fairall, 1986)

1. In the mixed layer, C = C_r

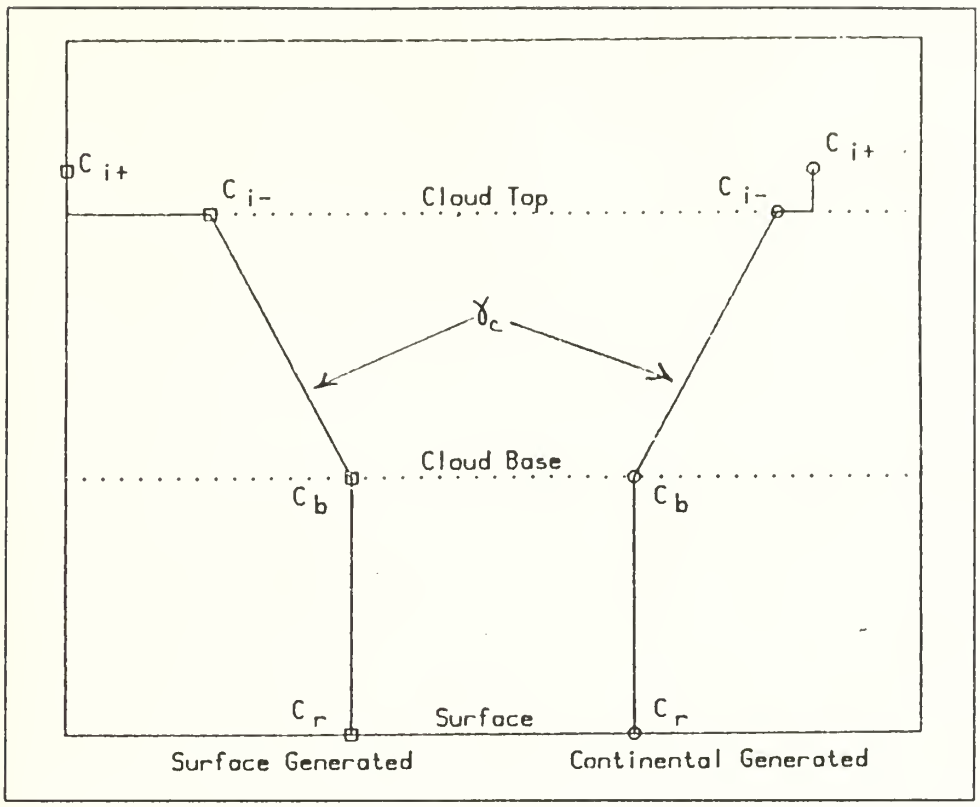

Figure 7. Schematic diagram of aerosol concentration: Dry aerosol concentration based on maritime and continental sources for a weak cumulus convection boundary layer structure. (Gathman, 1989)

2. In the cloud layer, $C = C_b^+ + \gamma_c(z - z_b)$
3. C_r is given by a standard wind speed dependent model
4. At the cloud top, assume:
   a. $C_i^+ = 0$ if C represents a locally generated sea-salt mode
   b. C_i^+ is given by climatology
5. $C_b^+ = C_b^- = C_r$

These assumptions lead to the following equation for the vertical gradient from cloud base to cloud top:

$$\gamma_c = \frac{(C_i^+ - C_r)n}{(1+n)\Delta z} \tag{10}$$

where n is a dimensionless entrainment parameter at the cloud top given by:

$$n = \frac{4w'_e \times (\tau - \nabla \cdot \vec{V})}{\Delta z} \tag{11}$$

In this form, the entrainment rate at the cloud base and the cloud wall entrainment are not important. These simplifications may reduce the accuracy in the vertical representation of dry aerosol concentration, but this predicted vertical structure is a large first step in improving the exponential model currently in use. With mixing and entrainment controlled by the potential temperature and relative humidity profiles, a more accurate representation of the transport properties in the sub-cloud and cloud layers is obtained.

B. RELATIVE HUMIDITY EFFECTS IN NOVAM

Since aerosol particles attenuate energy in an amount proportional to their cross sectional area, any model requiring aerosol extinction calculations must take into account the effect of relative humidity on aerosol growth. Vertical changes in relative humidity become important when requiring slant-path aerosol extinction calculations for the weak convective region where relative humidity is expected to increase with height up to the cloud layer, then decrease gradually to top of the cloud layer. Figure 8 shows the effect relative humidity has on particle radius (represented by the ratio of the aerosol particle radius at the indicated relative humidity (r) versus the radius of the same aerosol particle at 0% relative humidity (r_o)). Fitzgerald found that pure NaCl particles experienced a sudden increase in size at some critical value of relative humidity (between 70 and 76% relative humidity as represented by the hatched area in Figure 8) whereas naturally occurring maritime aerosol particles show continuous smooth growth with changing relative humidity. This may be explained by the gradual deliquescence of soluble material which is present as a mixture of different salts.

Based on the information shown in Figure 8, Fitzgerald developed the following relationship:

$$\frac{r(S)}{r_o} = \left[1 + \frac{\gamma}{1 - S} \right]^{\frac{1}{3}} \tag{12}$$

where γ represents the air-mass characteristic and S represents the saturation ratio (for the purposes of this discussion, S can be assumed to be equal to RH / 100).

The relative humidity dependence in both NAM and NOVAM appears in the form of f_i in the equation for size distribution (Equation 3). As can be seen in Figure 8, when the relative humidity increases, deviation of the measured ratios from any theoretical

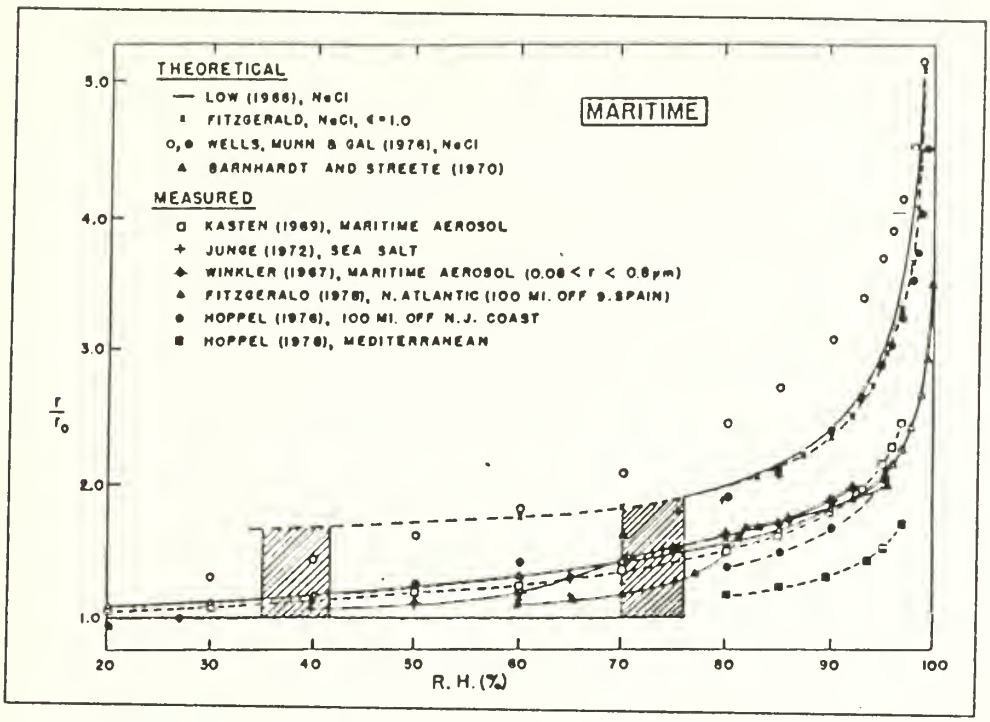

Figure 8. Growth curves for marine aerosols: Theoretical and calculated growth curves for NaCl particles and natural marine aerosols (Fitzgerald, 1978).

curve which is based on dry particle size becomes greater. Because relative humidity is generally above 50% throughout the MABL, a reference relative humidity of 80% was selected to minimize the error inherent in the theoretical aerosol growth calculation, and this reference relative humidity was used as a basis in computing f_i. An equation for f_i is generated by dividing equation 12 by the ratio of r(.8) to r_o yielding (Gerber, 1985):

$$f_I = \frac{r(S)}{r(.8)} = \left[\frac{C7_i - S}{C8_i(1 - S)} \right]^{\frac{1}{3}} \tag{13}$$

where C7, C8 are conditional constants based on the aerosol mode component (recall Figure 3 on page 7) as displayed in Table 3. To incorporate the fourth mode (mode 0) into Equation 3, simply change the summation to include modes 0 through 3.

Table 3. GROWTH FACTOR CONSTANTS AND VALIDITY RANGE

Aerosol Model Composition	Mode Component (i)	$C7_i$	$C8_i$	Range of Validity
Sea salt	3	1.97	5.83	RH < 99.99%
Sea salt	2	1.83	5.13	RH < 99.9%
Water Soluble	1	1.17	1.87	RH < 99%
Dust	0	$f_0 \equiv 1.0$		all values

V. THE KEY90 EXPERIMENT

A. GOAL

Most observational studies within the development of NOVAM have been accomplished off the California coast. Initial experiments involving the testing of NOVAM were performed in the same environment that the model was developed in. As expected, the model verifies reasonably well in that environment. Since NOVAM is intended to be a global maritime model, the model had to be tested in other geographical scenarios.

The KEY90 experiment was the first attempt to test NOVAM's performance in a tropic-like environment where shallow or deep convection exists. The shaded region in Figure 1, known as Marathon, was the region of data collection during KEY90. Insolation heating of the relatively shallow waters between Florida and Cuba causes convection to be the major meteorological process taking place near the air-sea interface in this region. Also, at Marathon data could be obtained by both boat and aircraft while being away from land influences and major continental effects on the data.

B. MEASUREMENTS

Simultaneous measurements were made of parameters that the model requires as inputs and of extinction profiles at various wavelengths. The extinction profile measurements are then compared to the results obtained by running NOVAM at wavelengths corresponding to those measured. The extinction profile measurements provided the standard to judge NOVAM extinction profile predictions. Although this procedure seems fairly straight forward, it is noted that it is difficult to provide an accurate estimate of either the measured extinction profile or of the quality of the meteorological data used as inputs to NOVAM (e.g. surface IR extinction @ 10.6 μm and a.m.p.).

The data measurements collected during KEY90 were made from shore, from a boat, and from two aircraft. Both the atmospheric surface layer and the MABL structures were probed in detail. Figure 9 shows the instrumentation involved in the experiment. For each instrument, an asterisk marks the days of operation. Instruments are grouped according to the information provided (i.e. air temperature, sea surface temperature, relative humidity, wind speed, wind direction, atmospheric pressure, visibility, vertical profiles, Lidar information, and other data). Table 4 gives a summary of the time and location that boat and aircraft atmospheric vertical profiles were taken. For easy refer-

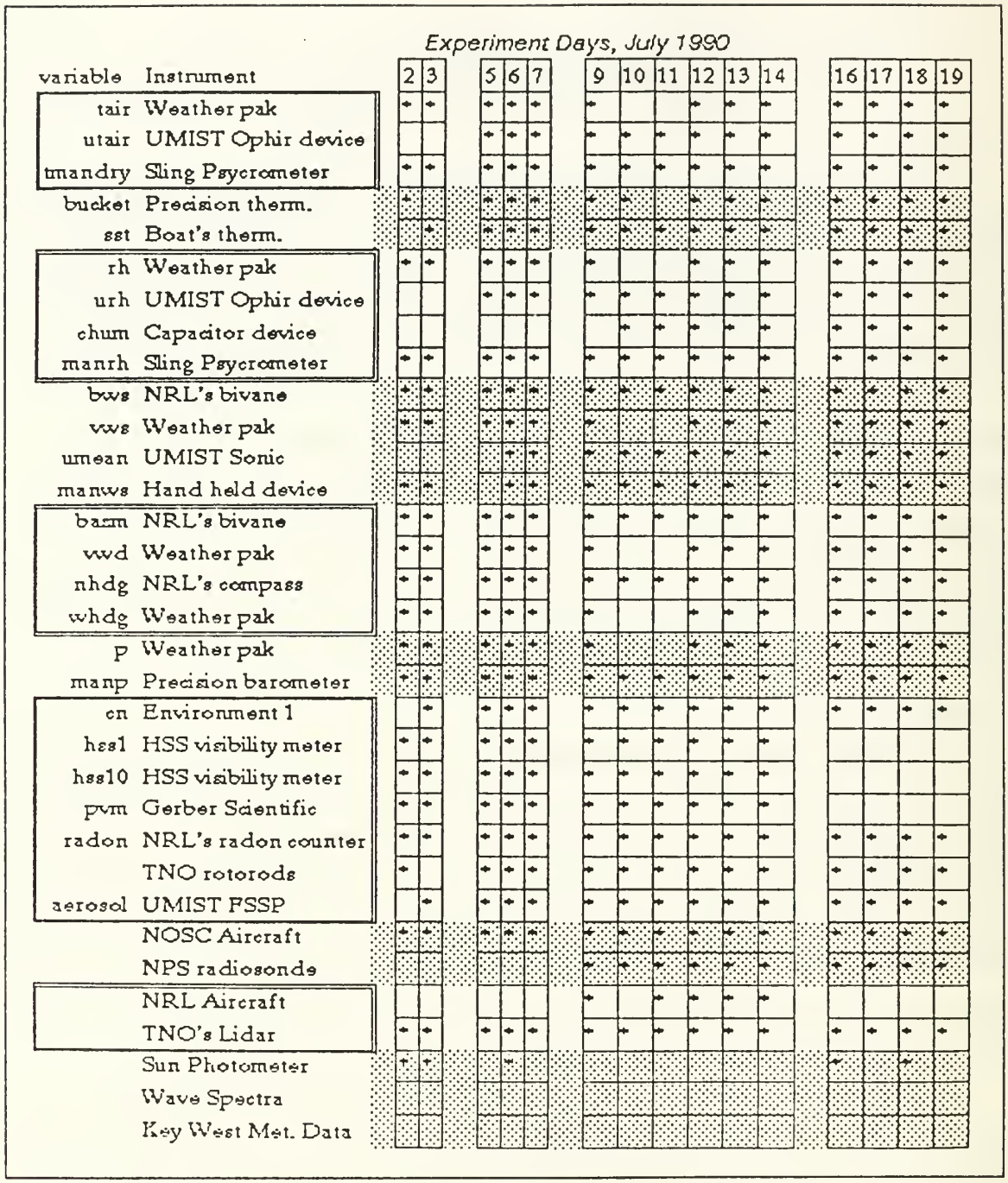

Figure 9. Summary of instrumentation used during KEY90: (Gathman, 1991)

ence, the difference of time (in minutes) and in location (in nautical miles) is provided in the last two columns.

Table 4. SOURCES FOR VERTICAL PROFILES

	Aircraft		Radiosonde			
Day	Time (UTC)	Location	Time (UTC)	Location	Δ t (min)	Δ x (n.m.)
09 Jul	2120	A	2200	24°13′N 80°33′W	40	23
10 Jul	2100	24°39′N 80°55′W	2200	24°23′N 80°33′W	60	25
12 Jul	0030	B	2330[1]	24°21′N 80°33′W	60	26
12 Jul	1930	B	1906	24°15′N 80°21′W	24	39
			1945	24°21′N 80°33′W	15	39
13 Jul	1330	B	1319	24°21′N 80°33′W	11	26
14 Jul	1140	B	1105	24°21′N 80°33′W	35	26
16 Jul	2100	A	2027	24°13′N 80°31′W	33	25
	2359	B	2324	24°21′N 80°32′W	35	27
17 Jul	1605	B	1617	24°36′N 80°53′W	12	2
18 Jul	1240	B	1218	24°30′N 80°53′W	22	5
	1545	A	1459	24°30′N 81°00′W	46	9
19 Jul	1020	B	1023	24°30′N 80°53′W	3	5

[1] 11 Jul
A = 24°22′N 80°55′W
B = 24°35′N 80°55′W

It should be noted that in the process of collecting data, areas of thunderstorm activity were avoided. This may have caused parameters such as average wind to be lower than what may have actually occurred.

C. ATMOSPHERIC SYNOPTIC SCALE

The major synoptic flow patterns which influenced conditions in the Marathon region from 9 to 19 July are shown in Figure 10. For the period of 9 - 10 July, surface winds at Marathon were generally from the east to south-east with speeds of approximately 5 m/s. This was a result of the influence of high pressure centered off the east coast of the U.S. (Figure 10a). The high pressure system continued to control the Marathon region winds on the 11th and 12th of July, however, short wave troughs were analyzed as passing through Marathon on 11 July.

As the high pressure system moved to the north-east, winds at Marathon shifted from east-southeast to a more southerly direction (Figure 10b). Wind speeds were be-

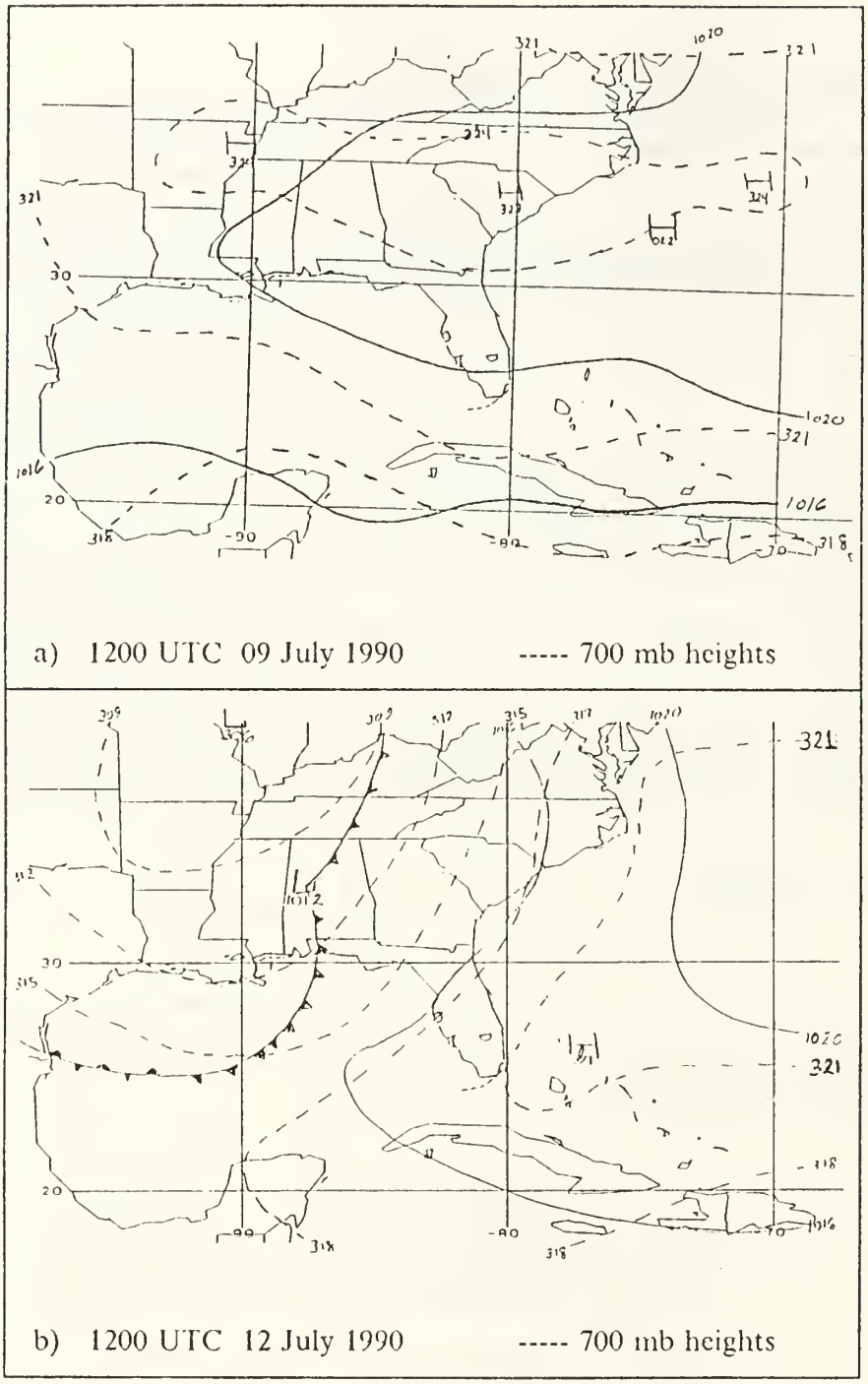

Figure 10. Synoptic pattern in Marathon area: Surface pressure (mb) and 700 mb heights (m * 10^{-1}) from NMC analysis for 1200 UTC is provided for the following days: a)9 July b)12 July.

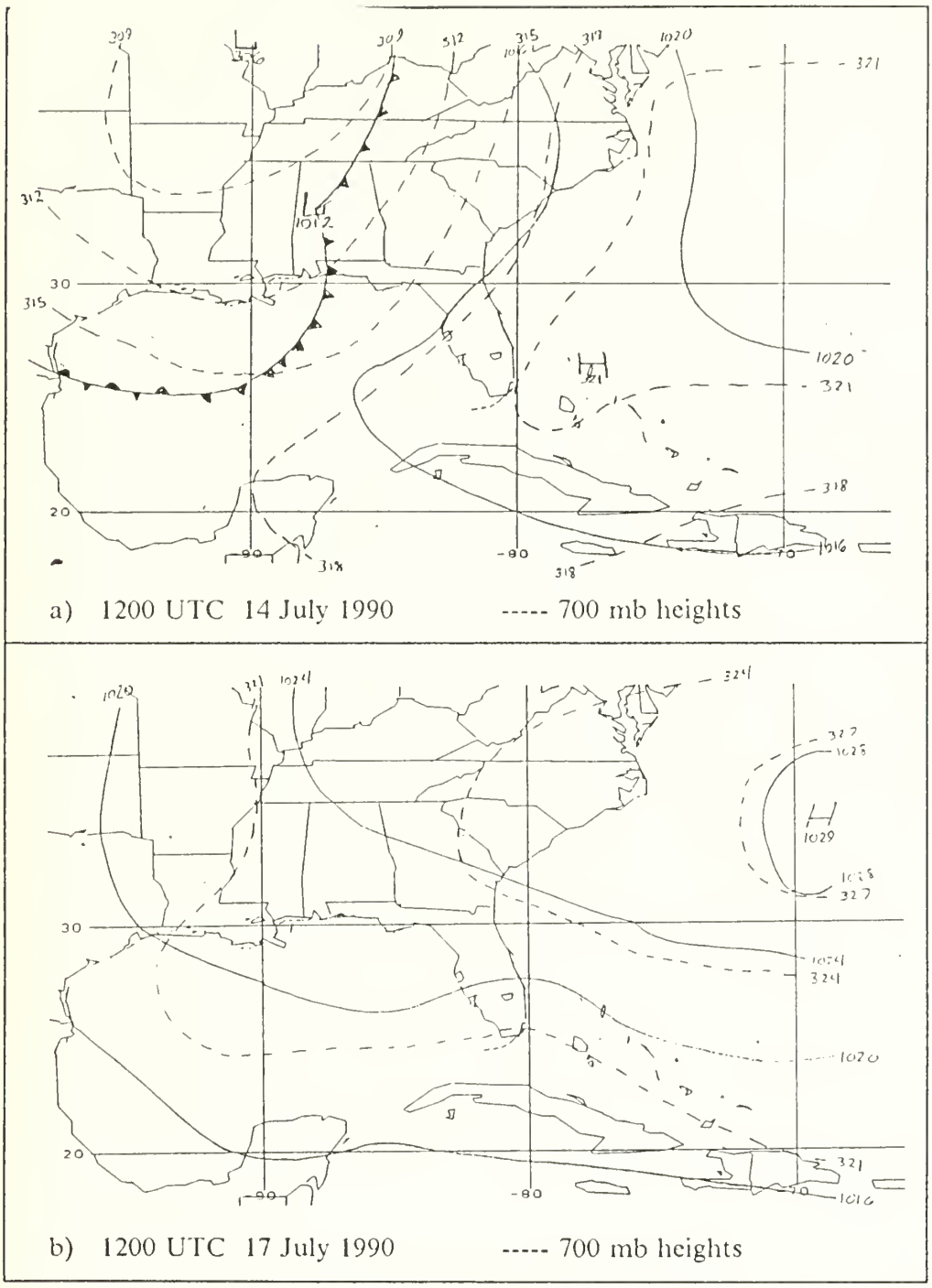

Figure 11. Synoptic pattern in Marathon area (cont.): Surface pressure (mb) and 700 mb heights (m * 10^{-1}) from NMC analysis for 1200 UTC is provided for the following days: a)14 July b)17 July.

tween 3 and 5 m/s during this period. By 13 July, a low pressure system which was approaching the eastern U.S. had an influence on winds at Marathon. Wind flow remained southerly, but wind speed decreased slightly due to weaker pressure gradients over the area. On 14 July, the low pressure center had deepened and moved to the east (Figure 11a). Surface wind flow over Marathon remained southerly with wind speeds increasing to 6 - 8 m/s. The cold front associated with the low pressure system was moving very slowly to the east. By late UTC on this day, it was evident that the frontal system was losing its upper level support, and the high pressure evident at 700 mb near the Florida Keys in the figure continued to build.

From 15 to 19 July, high pressure once again dominated the flow pattern in the Marathon region (Figure 11b). As the high pressure center moved to the north-east, the pressure gradient at all levels weakened. Surface winds were from the east to south-east throughout this period with wind speed decreasing to approximately 5 m/s by the 19th. A series of short-wave troughs were analyzed as passing through the Marathon region on 17 July.

Although all observations during KEY90 fell within the realm of weak convection defined by NOVAM, there were examples of deep convection in the form of thunderstorms. Thunderstorm activity was observed in the Marathon region on 14, 16, 17, and 19 July.

VI. NOVAM USAGE, PROCEDURE AND RESULTS

A. PROCEDURE

1. Surface File Generation

Each radiosonde and flight spiral profile requires corresponding surface file. Figure 9 shows that there were many choices for most surface file parameters. Because of consistent performance during the entire experiment, WeatherPak measurements were used for surface layer air temperatures, wind speeds, and relative humidities. When this information was not available on 10 and 11 July, sling psychrometer measurements were used for air temperature and relative humidity while a hand held device was used for wind speed. Bucket thermometer measurements of sea surface temperature were used. NRL's radon counter was used to establish the air mass parameter. The NOSC aircraft aerosol spectra was used to obtain the 10.6 μm aerosol extinction at the surface. The altitude of this reading was usually 30 meters above the surface. The optical visibility value was calculated by the model, based on the above parameters.

2. Radiosonde Preamble Generation

The general shapes of the potential temperature and mixing ratio (for flight) or specific humidity (for radiosonde) profiles were examined together when generating the radiosonde preamble. The first step was to establish heights of the first and second inversions (z_b and z_i in Figure 5). In general, a well-mixed layer was easy to establish below the first inversion, where potential temperature and mixing ratio remained constant. The more difficult task was determining a height for the second inversion. In most cases, there was no clear boundary (jump) to define the top of the cloud layer, especially in the potential temperature profiles. As a result, relative humidity profiles and observations of slope changes in the potential temperature and mixing ratio profiles were considered subjectively in making the determination.

3. NOVAM Runs

NOVAM runs for both the aircraft and radiosonde vertical profiles used the same surface file, so only one surface file was created for each row presented in Table 4. Information in the surface file is displayed above the radiosonde vertical profile panels in Figure 14 through Figure 26.

The jumps occurring between straight line segments of the radiosonde and aircraft profiles are important run parameters. The predicted amount of entrainment oc-

curring at the cloud top (second inversion) is dependent on the difference (jumps) in the potential temperatures and mixing ratios at the level. The smaller the difference, the more entrainment is occurring between the cloud layer and the layer above the second inversion. The wavelength of interest for each model run was an input parameter since aerosol extinction varies with wavelength. All the results presented in this thesis are for a wavelength of 3.5 μm, even though aerosol extinction profiles were obtained by NOSC aircraft at .53 μm, 1.06 μm, 3.5 μm, and 10.6 μm.

A NOVAM output file was generated for each vertical profile presented in Table 4. A separate run was also made to generate a limiting profile. For each surface file, the NOVAM default vertical profile was used with the relative humidity at each level set at 98%. When aerosol extinction measurements in the lower portion of the MABL exceed this value, precipitation is believed to be a possible cause, and the assumption of NOVAM that no precipitation exists is violated. The assumption of the default profile generator that each mode of the size distribution decreases exponentially with height will cause a difference in NOVAM versus limiting profile size distributions, increasing as the height of the well-mixed layer increases.

The importance of the relative humidity to aerosol extinction can be shown by comparing NOVAM profiles to limiting profiles. At a wavelength of 3.5 μm, an increase in relative humidity from the 80% typically observed at the surface to a 98% relative humidity (as used in the limiting profiles) results in an approximate order of magnitude increase in aerosol extinction prediction (comparison of aerosol extinction at surface between NOVAM predictions based on vertical profiles and NOVAM limiting profiles in Figure 14 through Figure 26). At the times of the vertical profiles, relative humidities above 90% were rarely seen, therefore a comparison could not be made of how well NOVAM actually performed at the higher relative humidities.

B. RESULTS

Simple comparisons between the flight and radiosonde potential temperature, mixing ratio, and aerosol extinction profiles reveal extensive variability in space and time. Results from 19 July (Figure 26) illustrate this point the best. From Table 4, the approximate horizontal distance between vertical profiles was five nautical miles, while the time difference was negligible. Analyses to determine the cloud-layer boundaries (defined by the first and second inversion) yielded a 150 meter difference in height of the cloud base and a 700 meter difference in the height that the second inversion occurred. The fact that there was a substantial spatial variability is further corroborated by the Lidar

extinction profile for 14 July shown in Figure 27, which clearly shows the spatial variation in atmospheric structure. As discussed above, slant-path calculations of transmittance currently assume aerosol extinction to be horizontally uniform. This condition does not appear to exist in the KEY90 region. A predicted aerosol extinction profile generated by NOVAM based on one vertical profile will most likely not be representative of the average vertical structure over the path of interest. In order for NOVAM to provide the required predictions, either the mean cloud base and cloud top levels over the path need to be established, or a technique needs to be developed to minimize the importance of the analyzed inversion levels.

All NOSC aircraft aerosol extinction observations between 9 - 19 July were plotted simultaneously (Figure 12) to examine how well NOVAM predictions characterized aerosol extinction. A subjectively determined mean profile was generated from the plots in Figure 12, and will be referred to as the flight composite. To be considered successful, separate NOVAM predictions should compare favorably to the flight composite under most circumstances. Due to space and time differences between the flight profiles and the radiosonde profiles, only NOVAM results from flight profiles were used in the comparisons with the observed aerosol extinction profiles. When considering only the top row of Figure 14 through Figure 26, the following features can be seen:

1. NOVAM aerosol extinction predictions above the second inversion were extremely poor.
2. Below the second inversion, NOVAM predictions compared favorably with the flight composite except in the cases where aerosol extinction dropped off noticeably (an order of magnitude difference between the surface and cloud base observations) below the cloud base (see top panel Figure 17c, Figure 20c, Figure 24c, and Figure 25c).

The assumption that aerosol extinction above the second inversion is essentially zero when the air mass parameter is calculated to be approximately equal to one does not appear to be a good one for this region. Aerosol extinction was determined to be significant if it is within one order of magnitude of the aerosol extinction that NOVAM calculates at the surface for the wavelength of interest. Using this as a criteria, the 12, 13, 14, 17, and 18 July NOVAM flight profiles all showed significant aerosol extinction contributions above the second inversion.

One possible explanation for the poor performance of NOVAM above the second inversion is that the weak or shallow convection assumptions are not effective here ,i.e. this may be a case of deep convection. Thunderstorm activity and rain were frequently observed in Marathon, and multiple cloud layers were not uncommon. The hypothesis

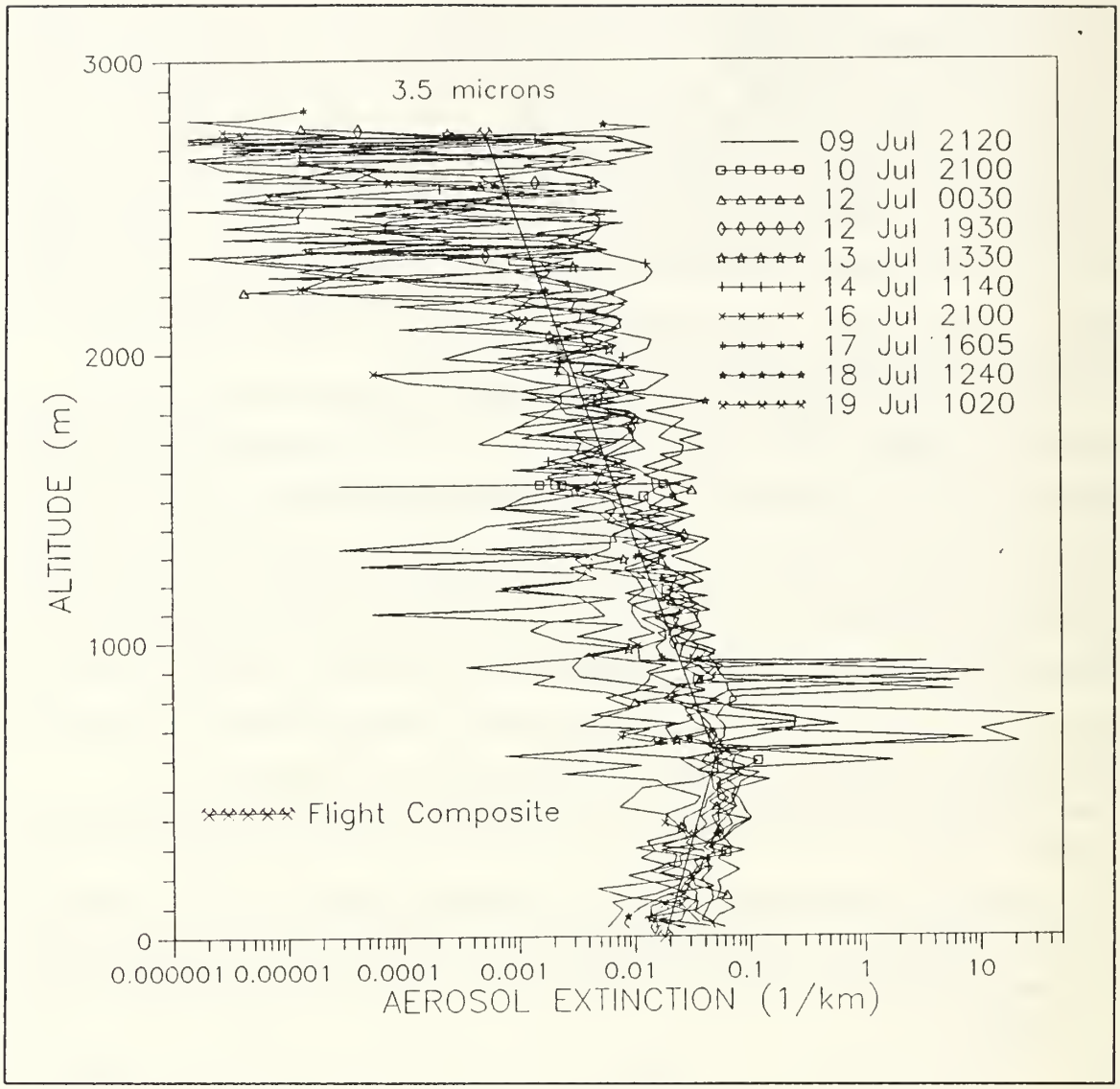

Figure 12. Flight extinction profiles with flight composite:

is that relatively small regions of deep convective activity result in an increased production of aerosol at the surface and transports aerosol to higher levels. As these deep convective cells dissipate, large amounts of aerosol are still being transported horizontally throughout the region, which would account for the aerosol present above the second inversion in many cases.

Another possible explanation may be that the atmosphere above the second inversion commonly contains a significant number of small radii aerosol particles. These

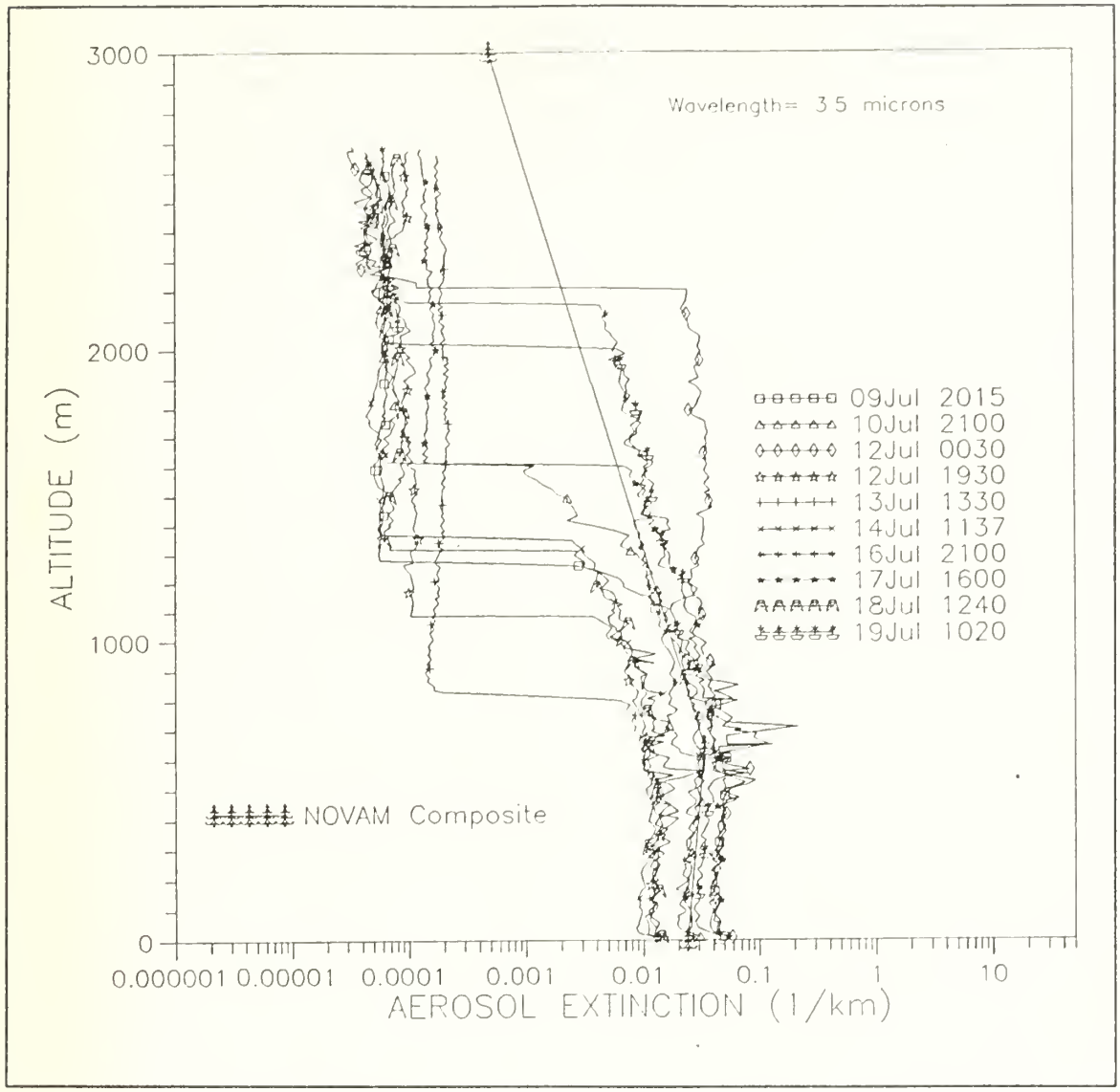

Figure 13. NOVAM prediction profiles with NOVAM composite:

particles may originate either from continental sources or from the ocean surface in the form of DMS. These DMS particles would be carried to the upper atmosphere by convective cells and transported by large scale circulation. Particle processes associated with DMS origins are not well understood. (Durkee et al., 1990)

If the predicted aerosol extinctions above the second inversion are ignored, and a simultaneous plot of NOVAM predictions based on flight vertical profiles is made, a NOVAM composite can be obtained (Figure 13) in the same manner as the flight

composite described above. The flight and NOVAM composites turned out to be nearly identical (Figure 14c). There was not much variation in wind speed at Marathon and no frontal systems passed through during the KEY90 experiment, therefore it is likely that aerosol generation and transport mechanisms remained fairly constant during KEY90. This would explain why composite mean profiles performed as well as NOVAM predictions below the second inversion. It is possible that mean profiles, such as the composites generated above, can characterize the typical aerosol extinction (at a 3.5 μm wavelength) for the Marathon region during July. This approach leads to the region being described empirically, therefore the predictions are specific to one region during one season. The required data base for describing all ocean regions for each season would be enormous and the time and expense involved would be substantial.

The fact that a simple exponential curve developed from composite mean profiles performed much better than NOVAM above the evaluated second inversion indicates a need for further research on aerosol size distributions in the upper atmosphere. If the structure observed in KEY90 is in fact due to deep convective processes, a revision would have to be made to the sub-model selection process in NOVAM. Also, instead of the weak-convective assumption that the mode 2 and 3 components drop off to 0 above the second inversion, an exponential function could be used to describe the aerosol size distributions for these modes.

It is believed that the observations where aerosol extinction decreased noticeably below the first inversion are attributed to the combination of increased aerosol production at a time prior to the observation, possibly caused by thunderstorm activity, and scavenging in the lower layer due to rain, creating a deficit of aerosol below the cloud layer. If future experiments reveal that rain scavenging accounts for reduced aerosol extinction below the cloud layer, the present weather surface input file parameter is currently the only means that this information can be relayed to NOVAM. Because the aerosol extinction predicted at the surface is tied to surface observations of aerosol extinction, the task of modeling this phenomenon would still remain.

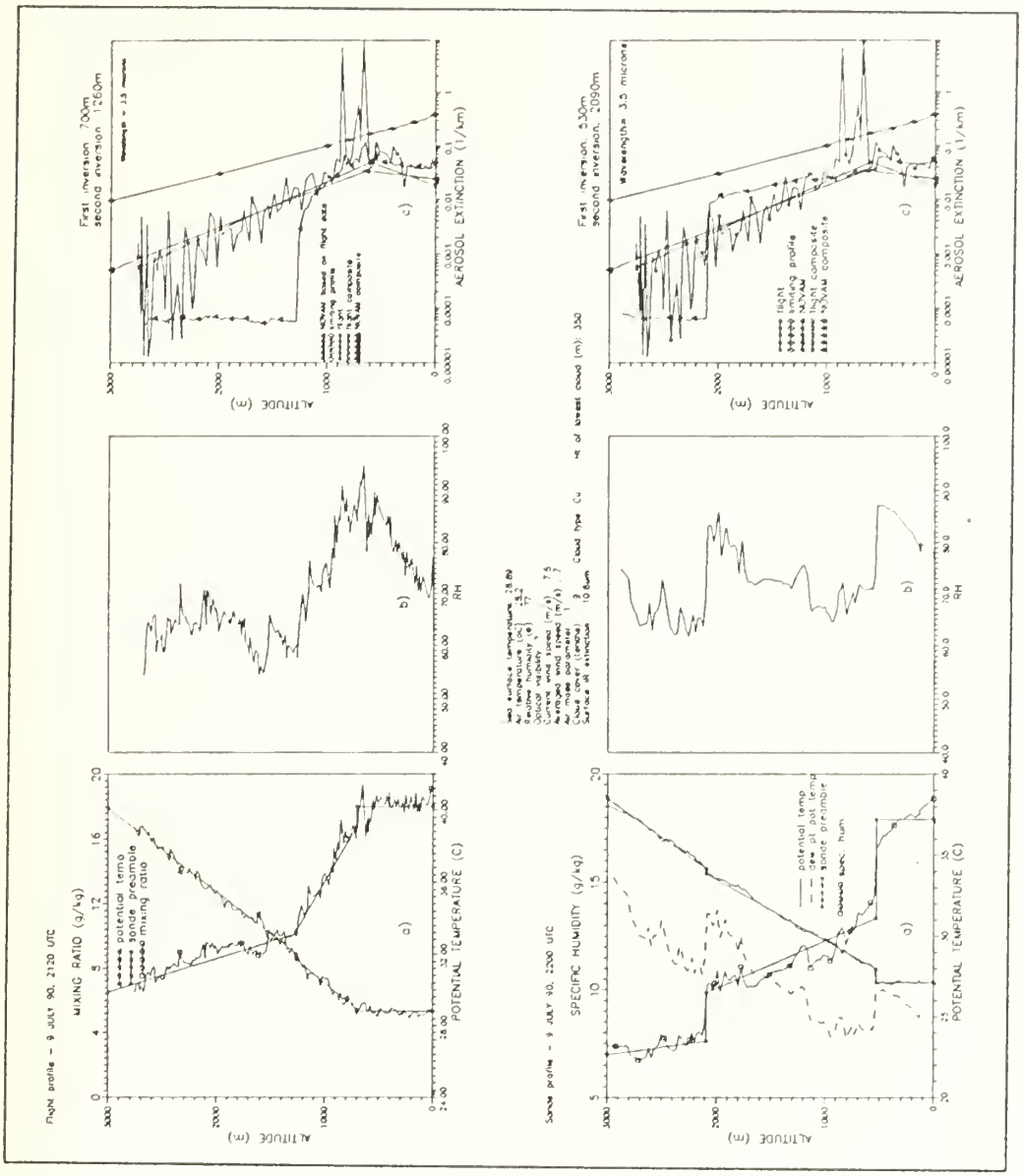

Figure 14. **9 July results:** The top panels are based on flight vertical profiles observed 09 July, 2120 UTC. Bottom panels are based on radiosonde profiles for 09 July, 2200 UTC. Panels labeled a) represent temperature and mixing ratio (flight) or specific humidity (sonde) versus altitude, b) plots relative humidity versus altitude, and c) shows aerosol extinction at 3.5 μm versus altitude. Refer to text for a description of the profiles appearing in panel c).

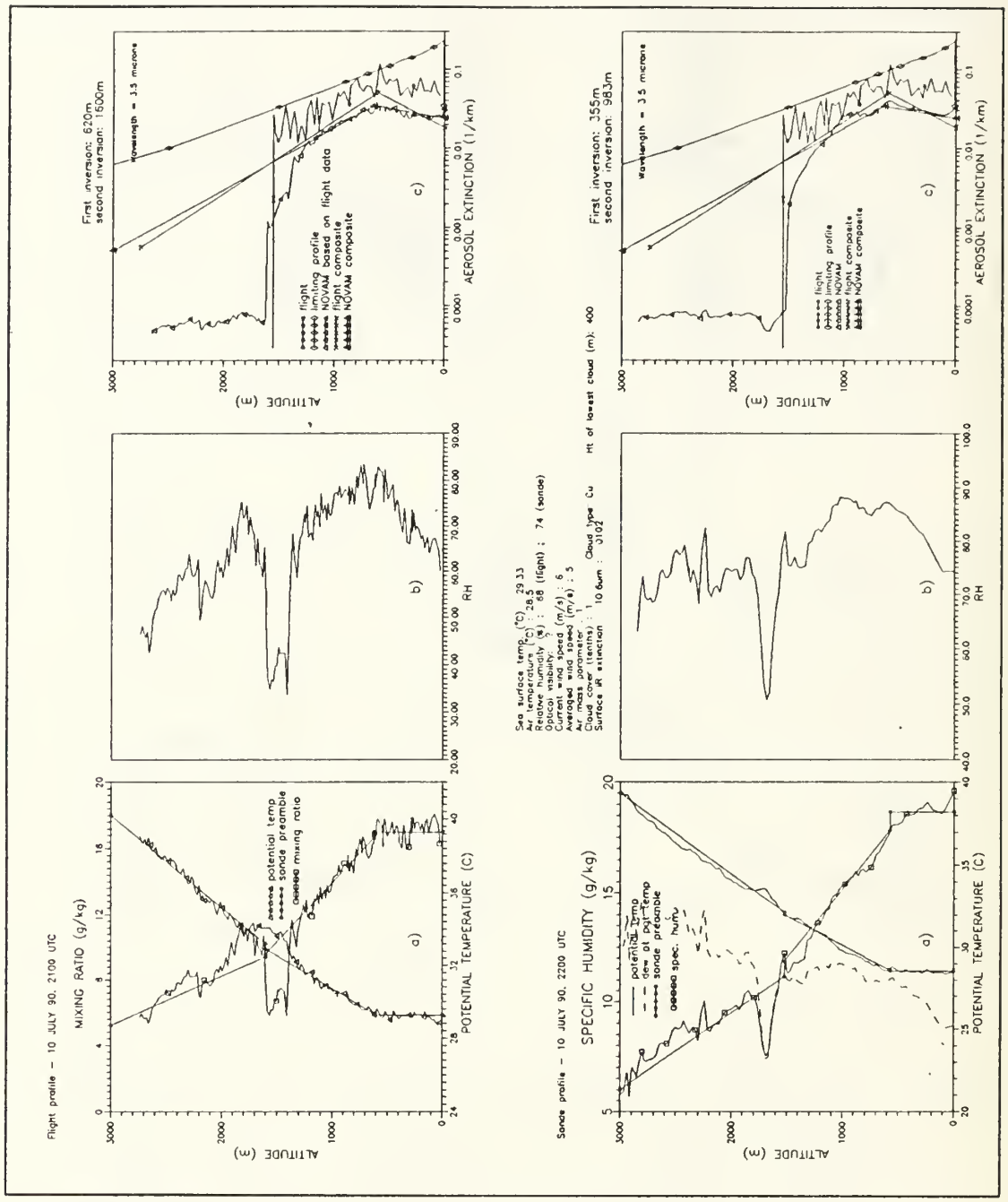

Figure 15. 10 July results: The top panels are based on flight vertical profiles observed 10 July, 2100 UTC. Bottom panels are based on radiosonde profiles for 10 July, 2200 UTC. Panel description is same as in Figure 14.

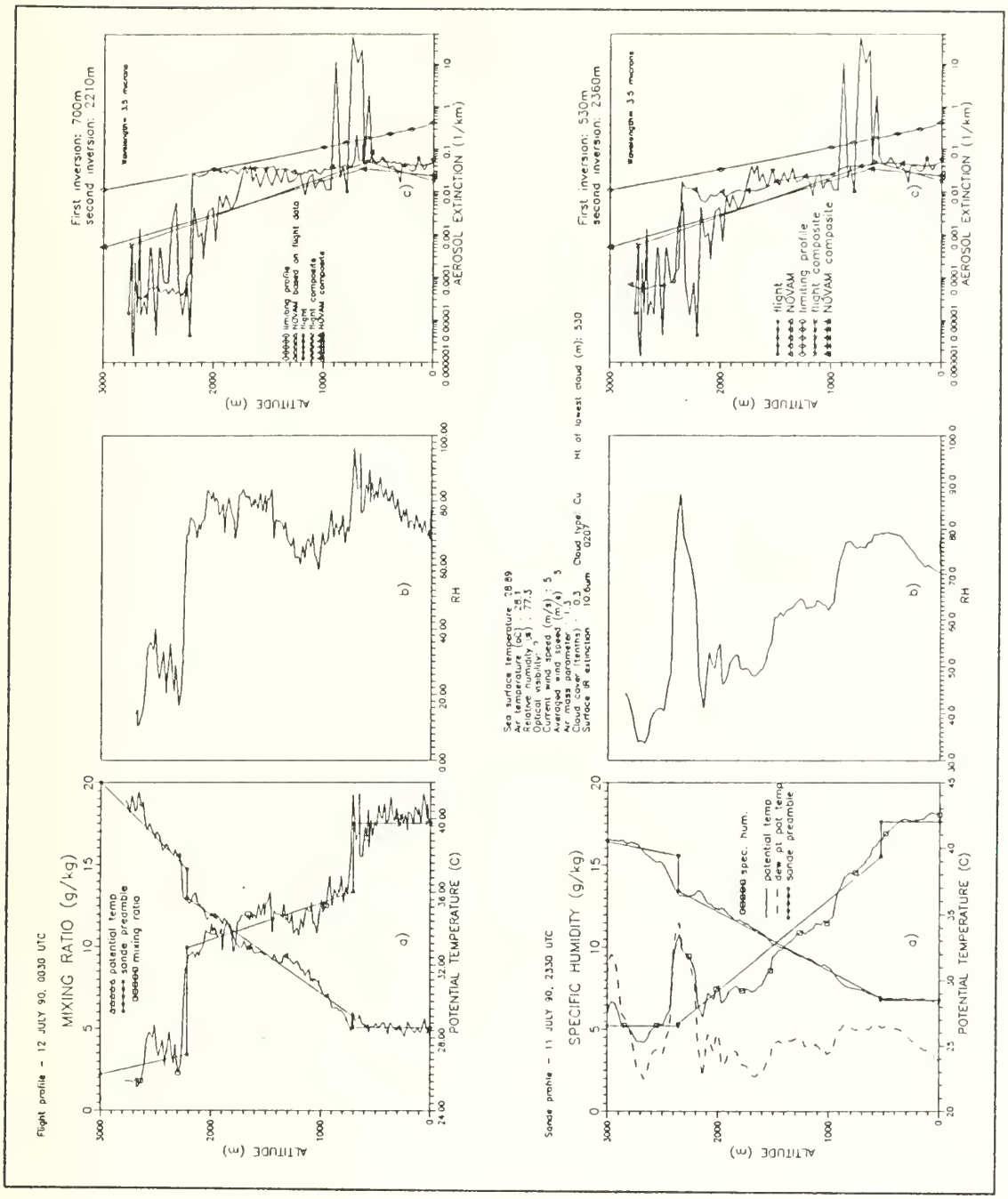

Figure 16. 12 July results for 0030 UTC: The top panels are based on flight vertical profiles observed 12 July, 0030 UTC. Bottom panels are based on radiosonde profiles for 11 July, 2330 UTC. Panel description is same as in Figure 14.

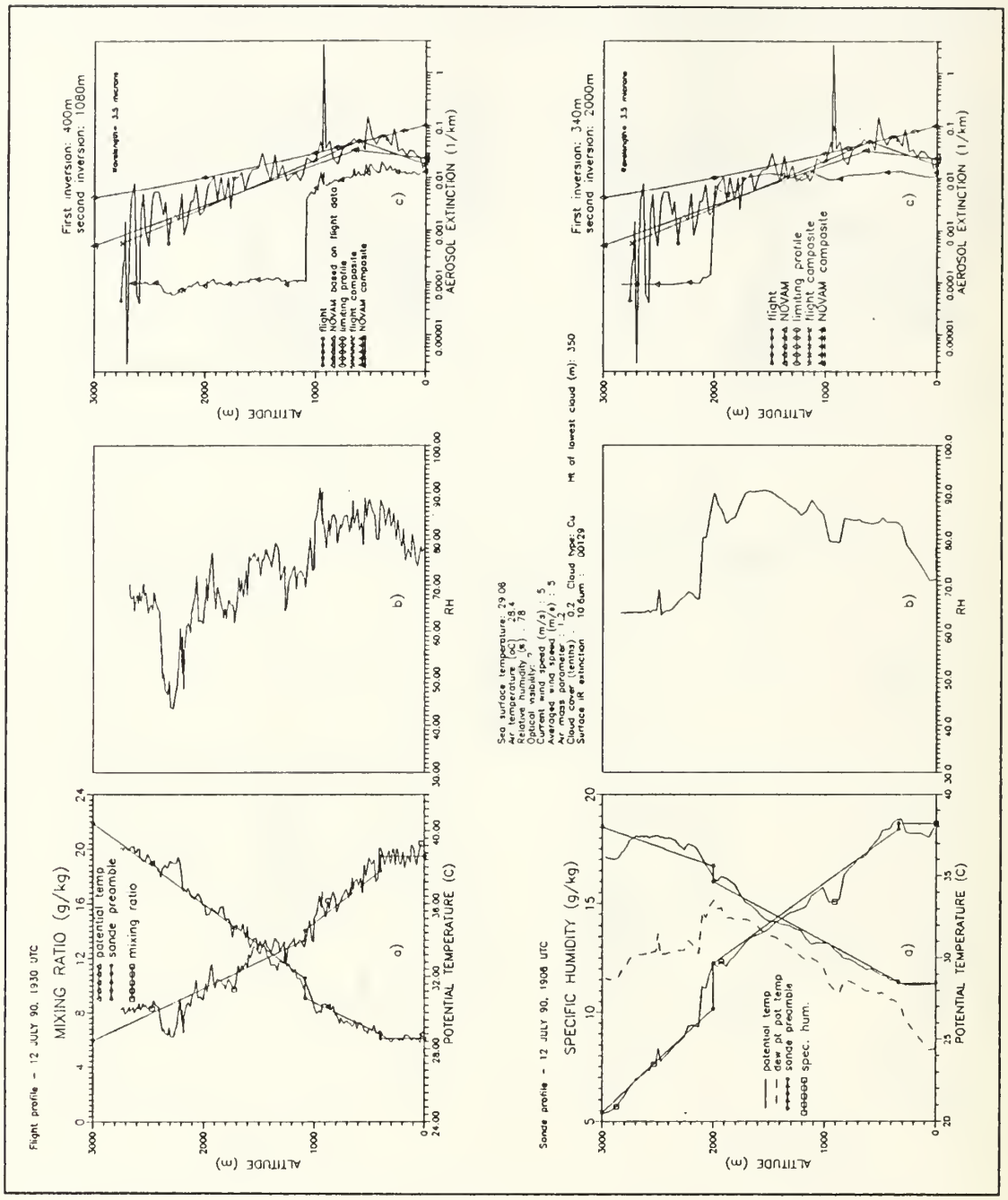

Figure 17. 12 July results for 1930 UTC (a): The top panels are based on flight vertical profiles observed 12 July, 1930 UTC. Bottom panels are based on radiosonde profiles for 12 Jul, 1906 UTC. Panel description is same as in Figure 14.

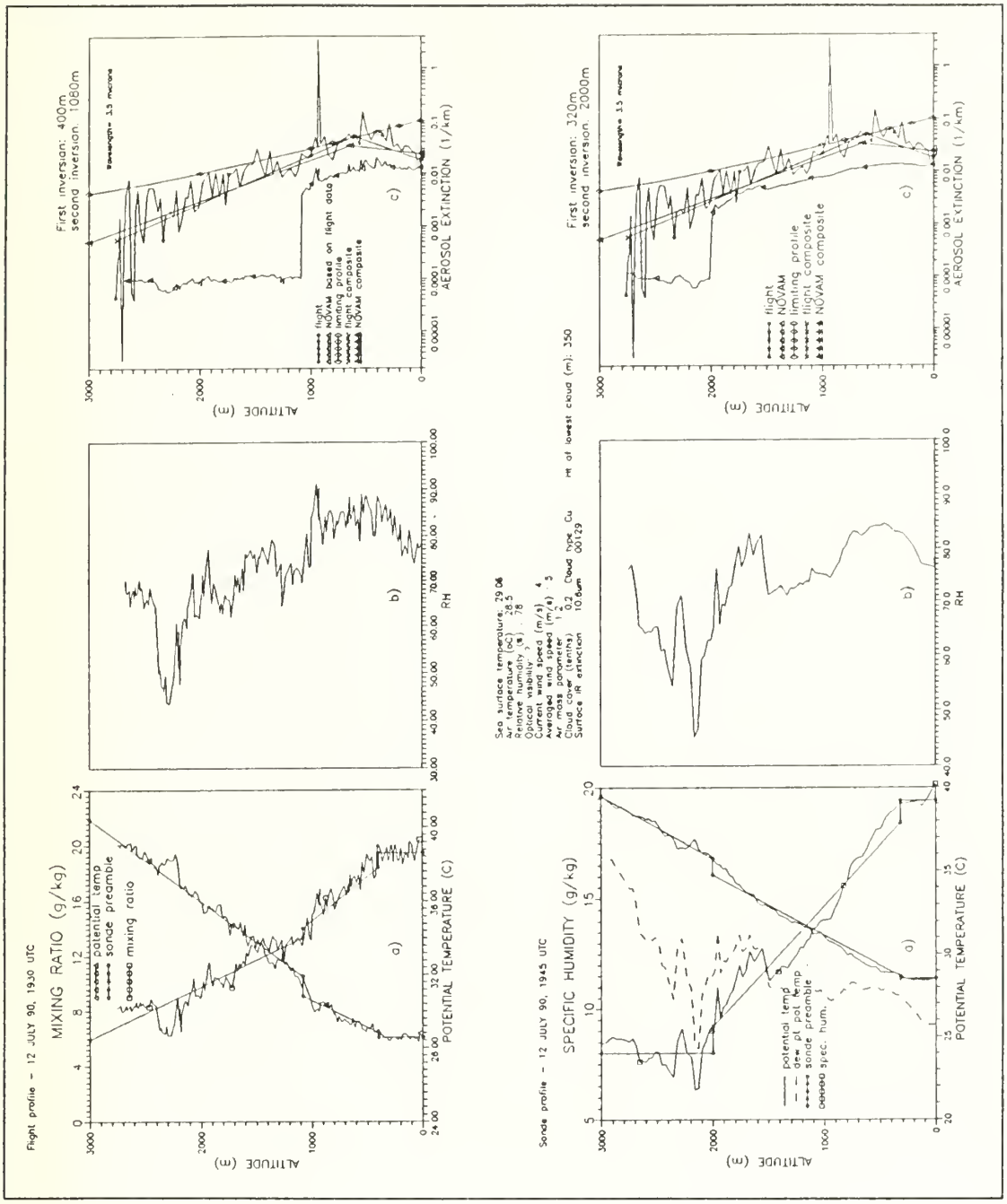

Figure 18. 12 July results for 1930 UTC (b): The top panels are based on flight vertical profiles observed 12 July, 1930 UTC. Bottom panels are based on radiosonde profiles for 12 Jul, 1945 UTC. Panel description is same as in Figure 14.

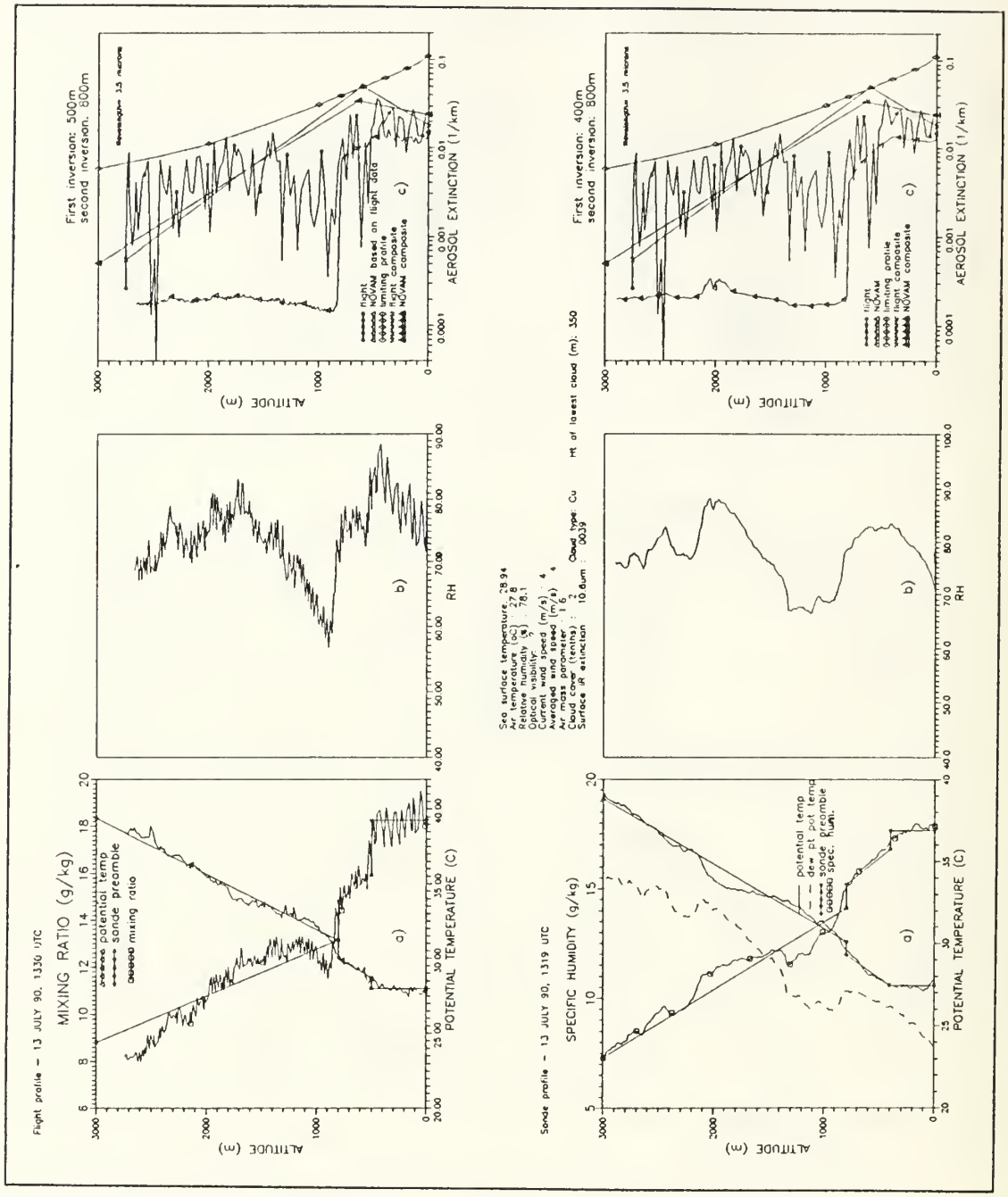

Figure 19. **13 July results:** The top panels are based on flight vertical profiles observed 13 July, 1330 UTC. Bottom panels are based on radiosonde profiles for 13 July, 1319 UTC. Panel description is same as in Figure 14.

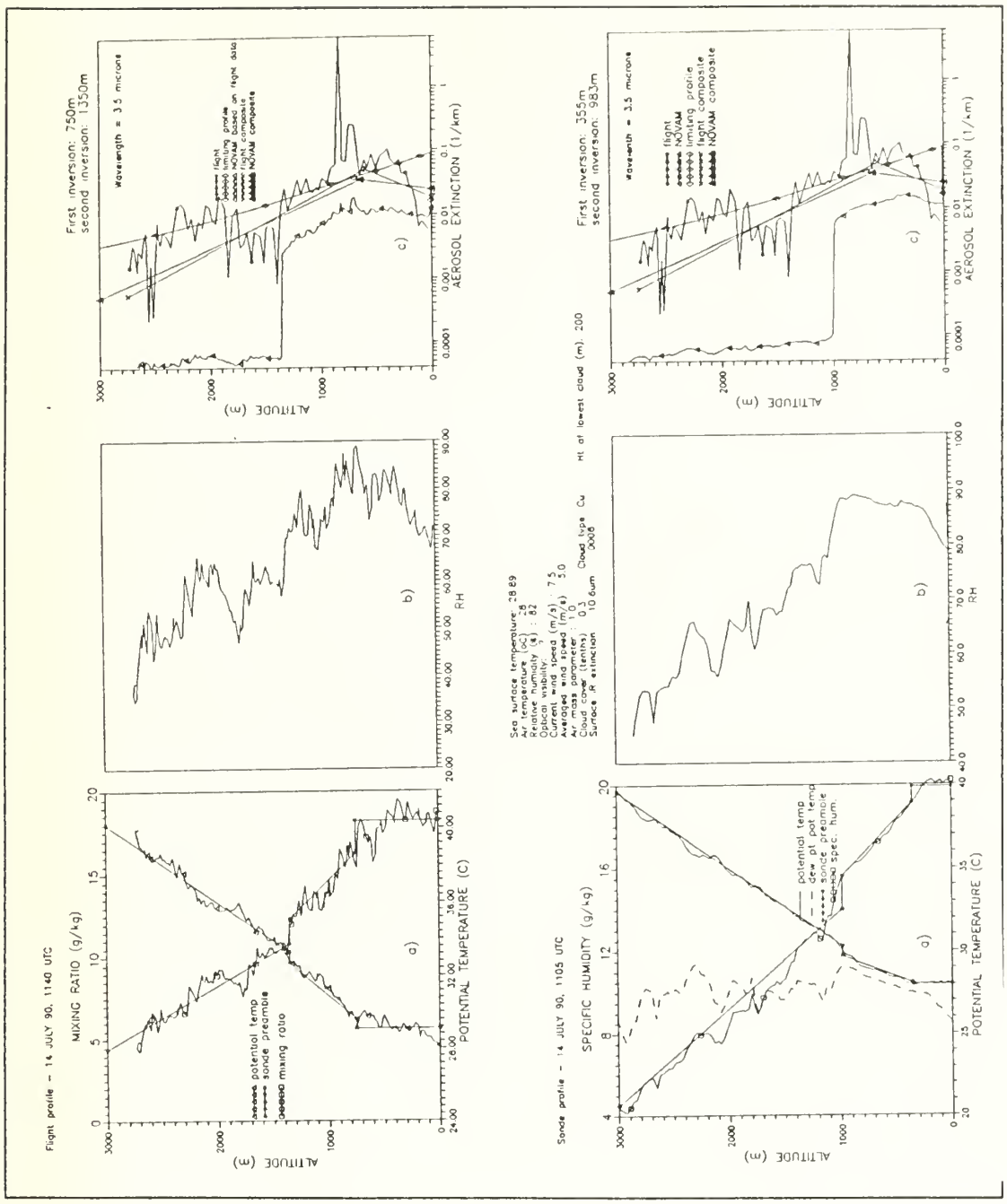

Figure 20. **14 July results:** The top panels are based on flight vertical profiles observed 14 July, 1140 UTC. Bottom panels are based on radiosonde profiles for 13 July, 1105 UTC. Panel description is same as in Figure 14.

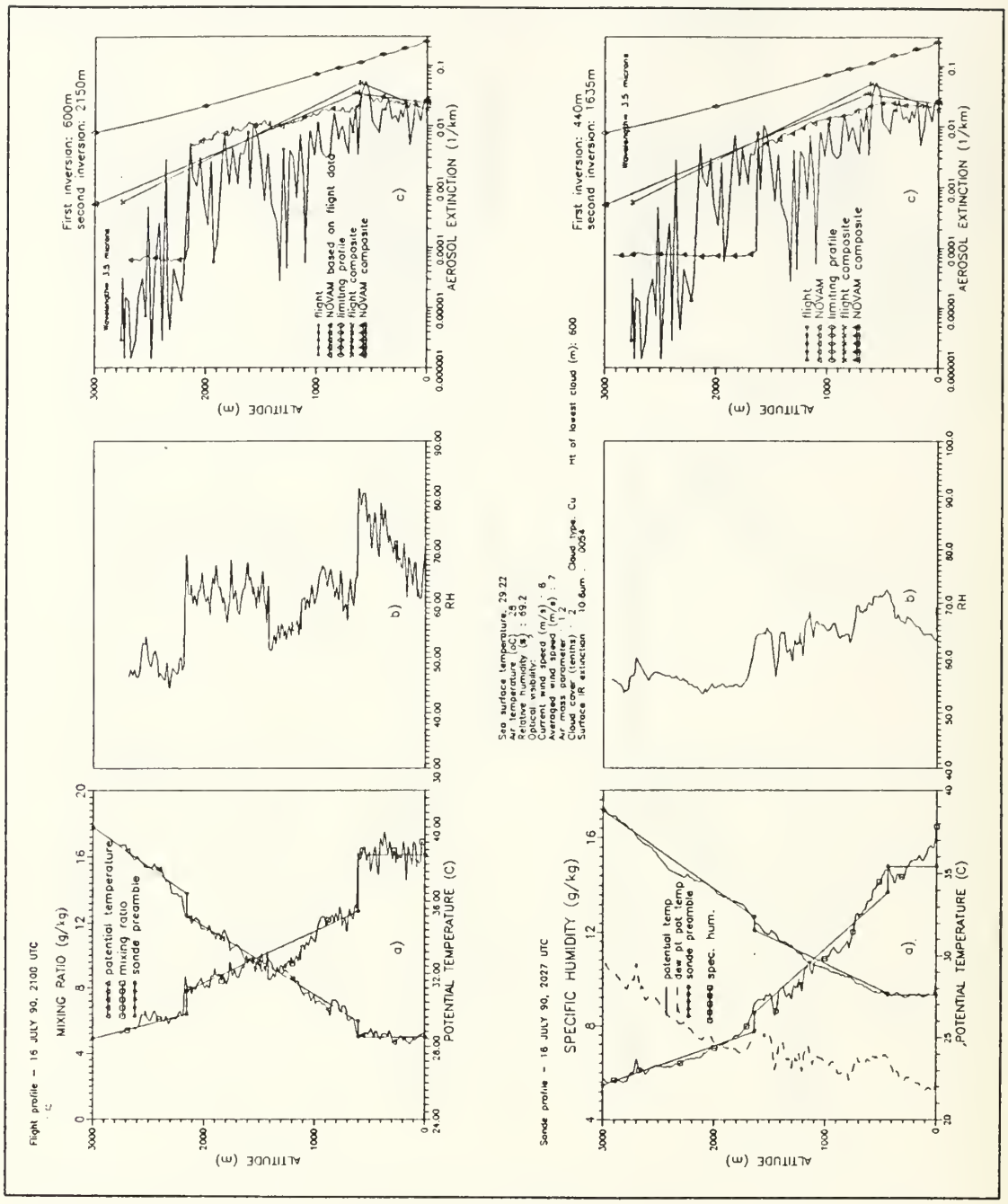

Figure 21. **16 July results for 2100 UTC:** The top panels are based on flight vertical profiles observed 16 July, 2100 UTC. Bottom panels are based on radiosonde profiles for 16 July, 2027 UTC. Panel description is same as in Figure 14.

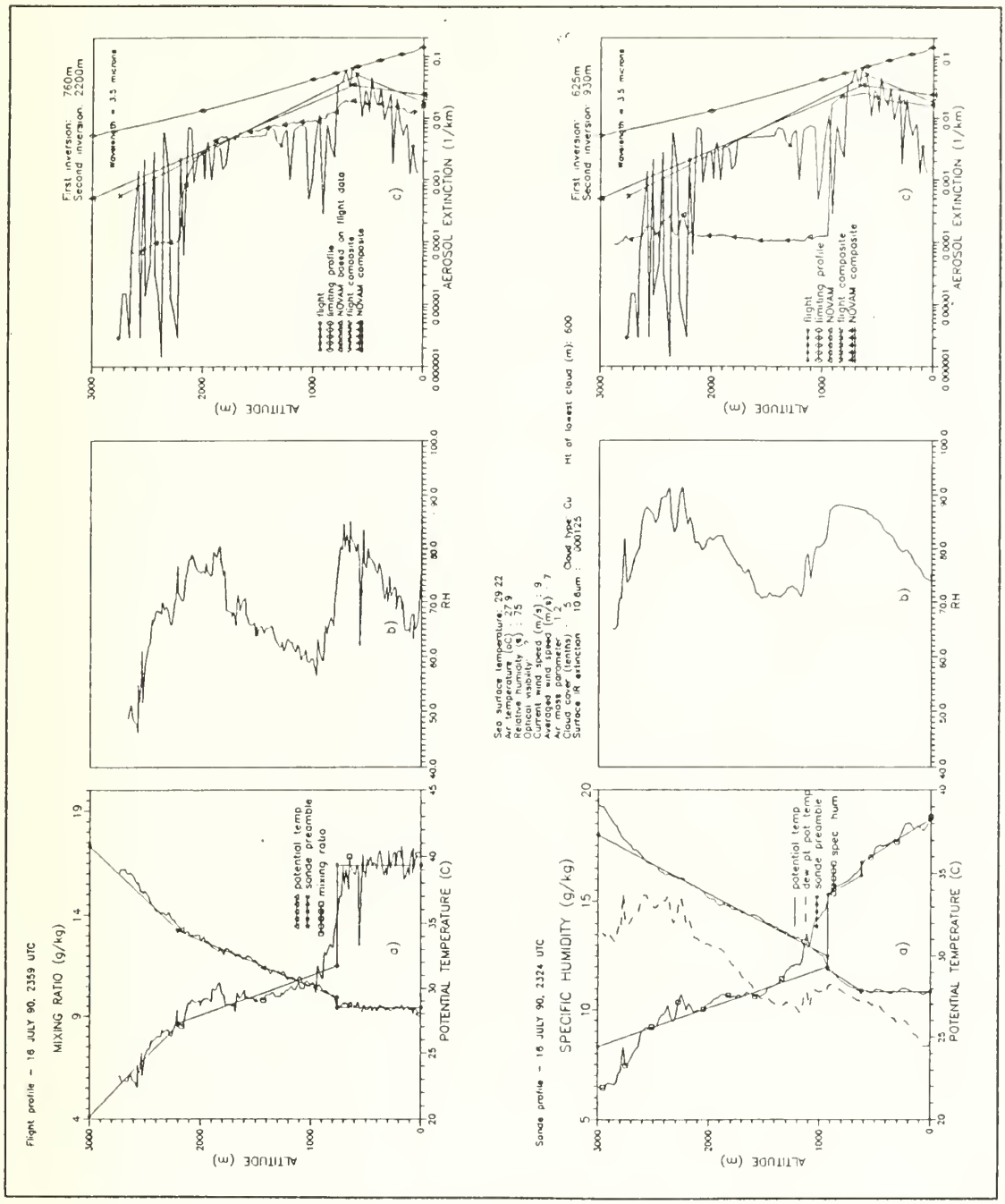

Figure 22. **16 July results for 2359 UTC:** The top panels are based on flight vertical profiles observed 16 July, 2359 UTC. Bottom panels are based on radiosonde profiles for 16 July, 2324 UTC. Panel description is same as in Figure 14.

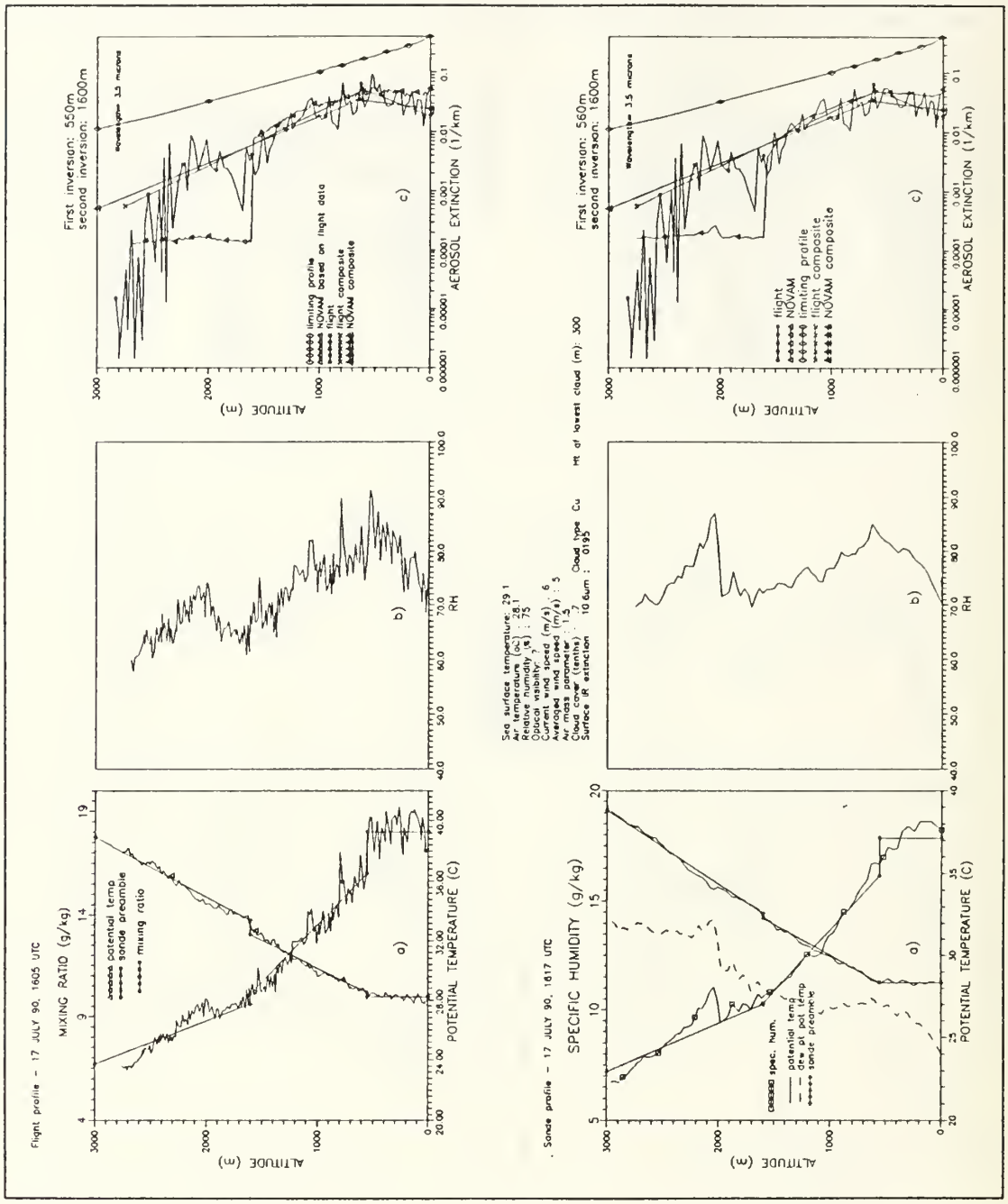

Figure 23. **17 July results for 1605 UTC:** The top panels are based on flight vertical profiles observed 17 July, 1605 UTC. Bottom panels are based on radiosonde profiles for 17 July, 1617 UTC. Panel description is same as in Figure 14.

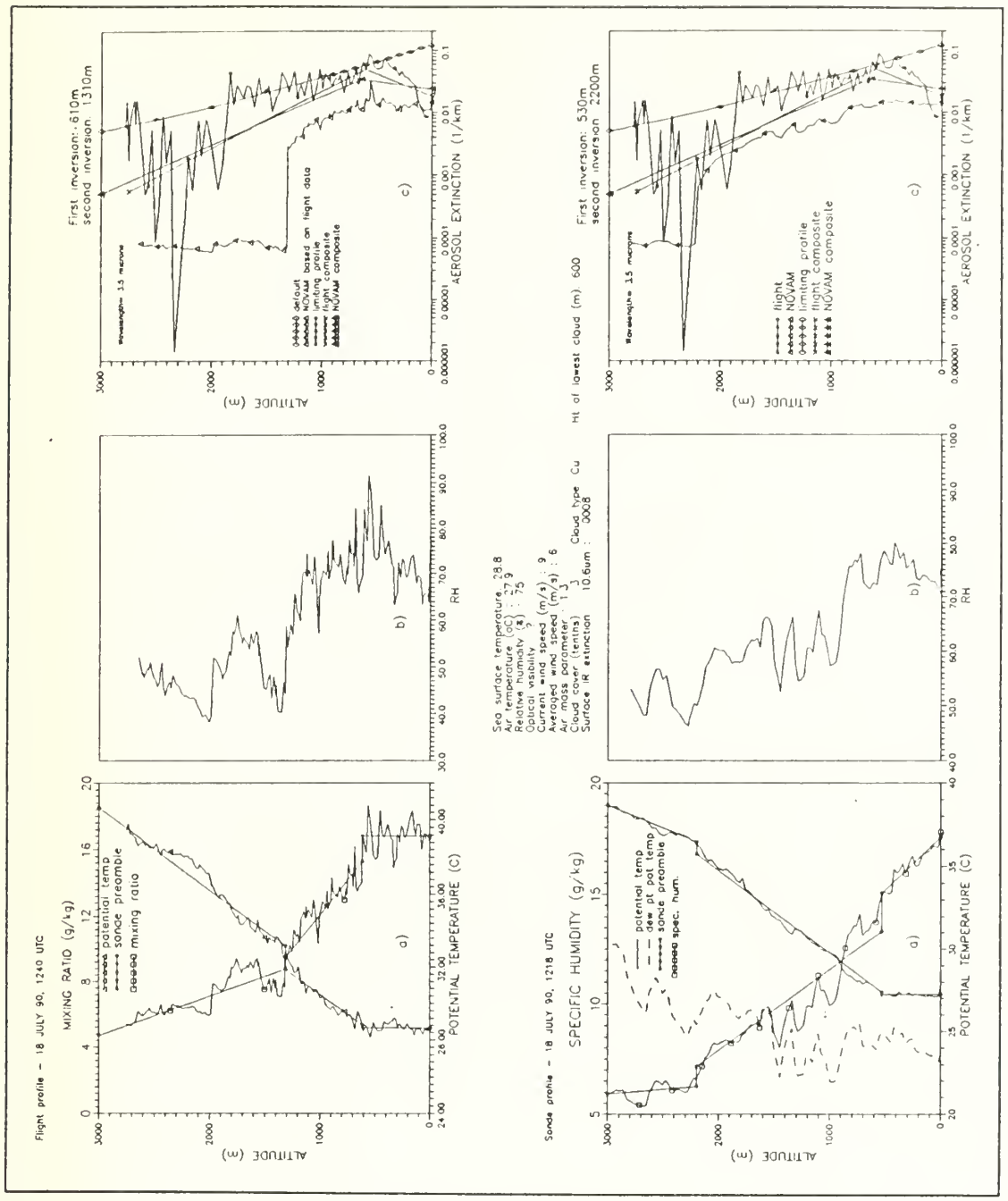

Figure 24. 18 July results for 1240 UTC: The top panels are based on flight vertical profiles observed 18 July, 1240 UTC. Bottom panels are based on radiosonde profiles for 18 July, 1218 UTC. Panel description is same as in Figure 14.

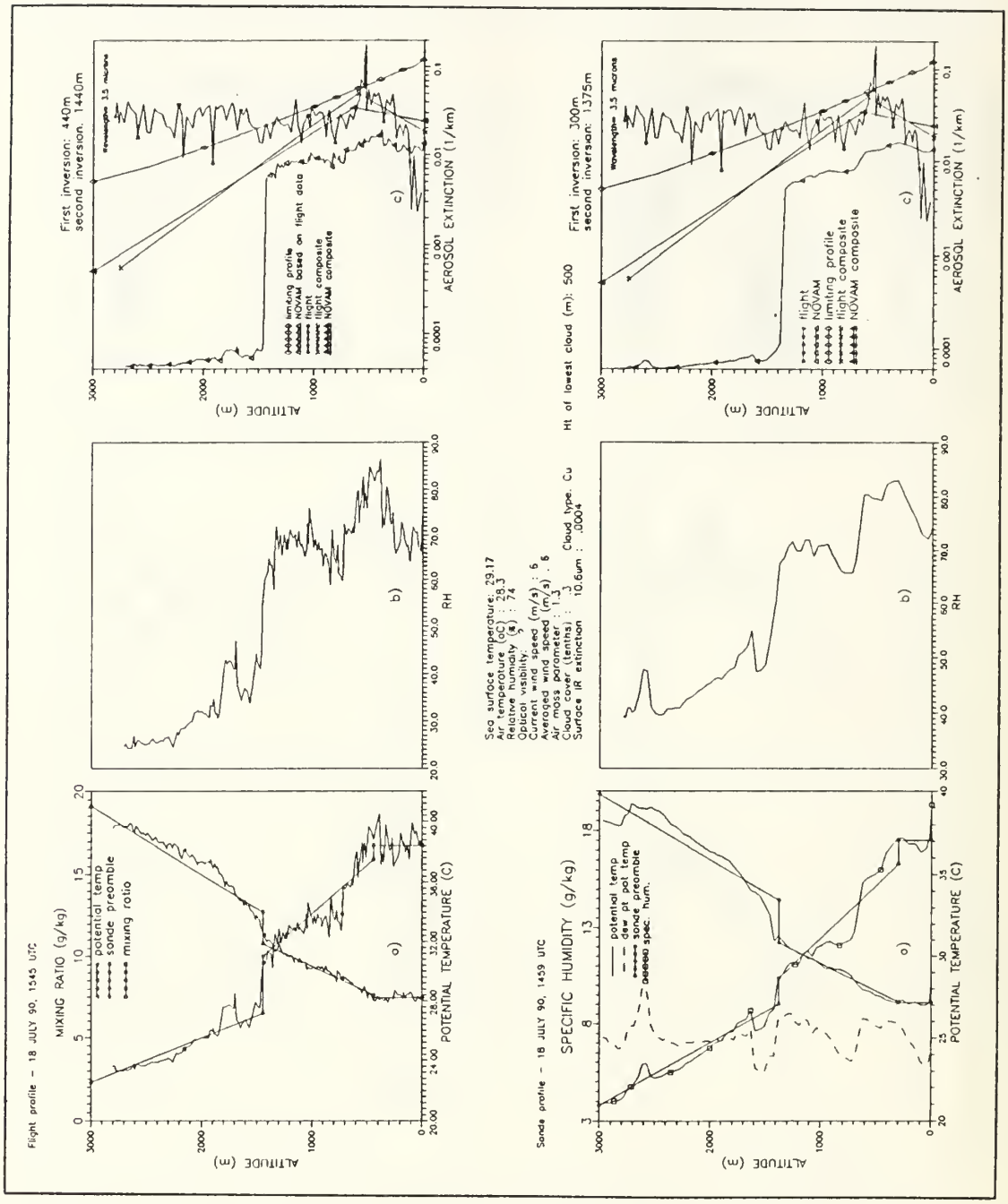

Figure 25. 18 July results for 1545 UTC: The top panels are based on flight vertical profiles observed 18 July, 1545 UTC. Bottom panels are based on radiosonde profiles for 18 July, 1459 UTC. Panel description is same as in Figure 14.

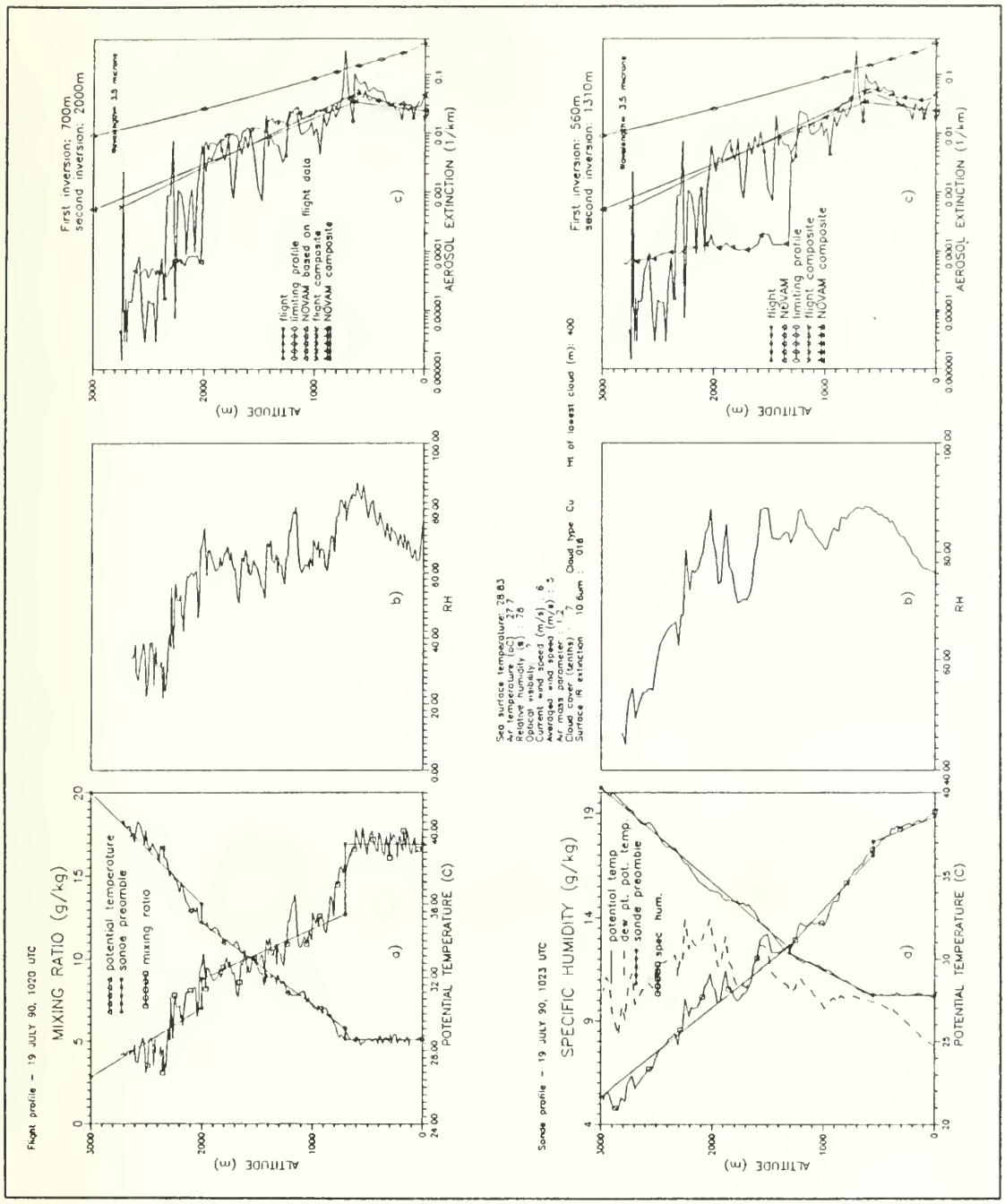

Figure 26. **19 July results:** The top panels are based on flight vertical profiles observed 19 July, 1020 UTC. Bottom panels are based on radiosonde profiles for 19 July, 1023 UTC. Panel description is same as in Figure 14.

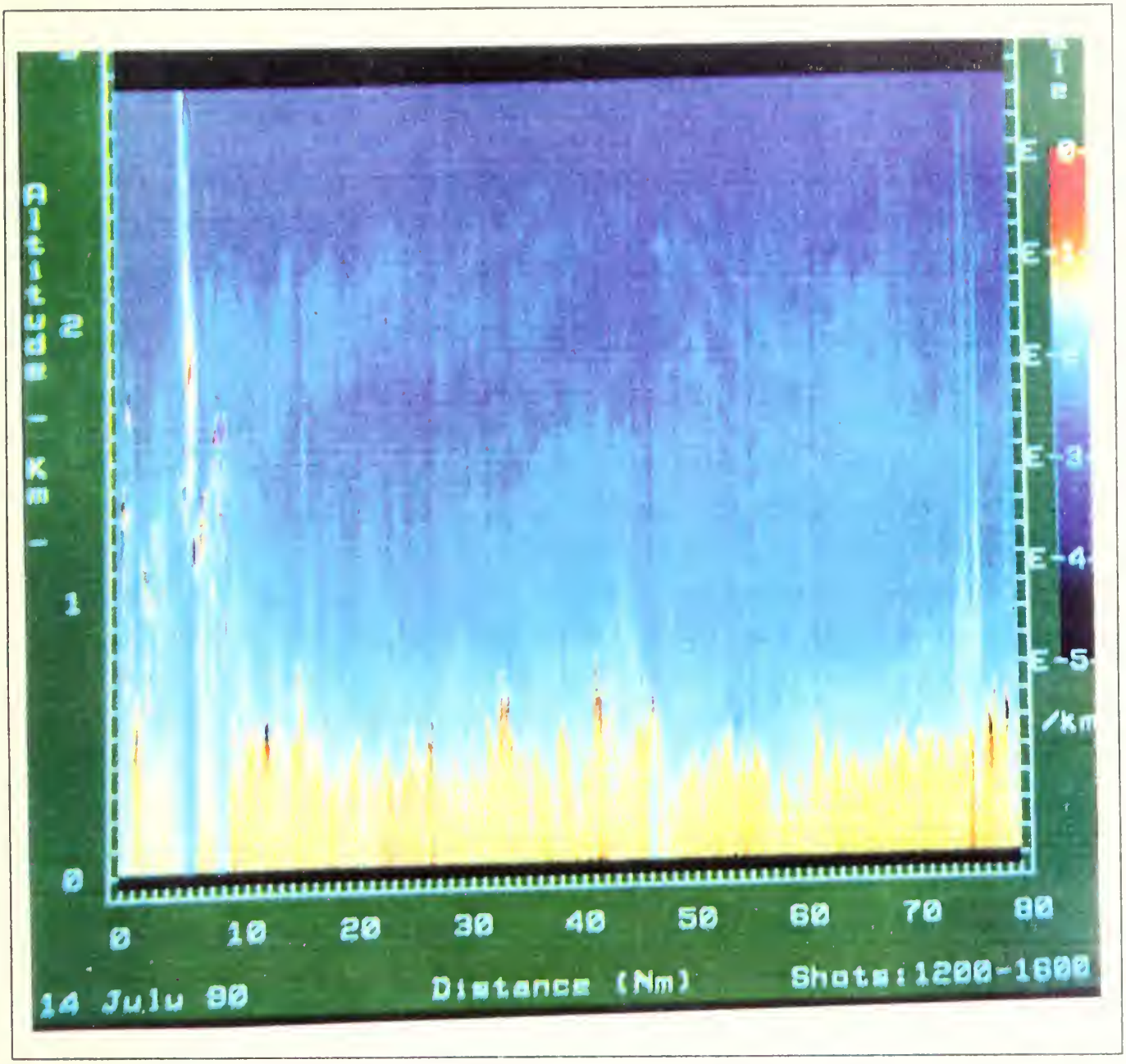

Figure 27. **Logarithmically amplified NRL Lidar extinction profiles:** Coded in false color, horizontal axis is distance covered by NRL aircraft from 1107 - 1126 UTC recorded on 14 July 1990. Vertical axis is altitude above sea level. Colors represent aerosol extinction in km^{-1} as given by the bar code on the right hand side. (Hooper, 1991)

VII. SUMMARY, CONCLUSION AND RECOMMENDATIONS

An experiment was conducted in the Florida Keys from 2 - 19 July 1990 to test the performance of the Naval Oceanic Vertical Aerosol Model (NOVAM) in a tropical, weak-convective regime. Meteorological data collected by aircraft and boat was used to generate the surface and vertical profile information files required by NOVAM. Using this information, NOVAM predicts the aerosol extinction (km^{-1}) for a vertical cross-section of the atmosphere. When NOVAM is incorporated into the LOWTRAN model, which also accounts for molecular extinction, slant-path calculations for transmittance may be performed.

Aircraft-observed aerosol extinction profiles were obtained in order to verify NOVAM predictions of aerosol extinction. Comparisons between observed and NOVAM aerosol extinction profiles revealed major deviations above the cloud top. From the surface to the top of the cloud layer, NOVAM generally did an excellent job in predicting profile shape, with the magnitude of aerosol extinction tied to the extinction matched at the surface. In a few cases, observed extinction increased more rapidly than NOVAM predicted extinction from the surface to the base of the cloud layer. This is attributed to rain scavenging associated with thunderstorm activity in the area. Comparison between different aerosol extinction profiles over time and space revealed much variation, which Lidar profiles of atmospheric structure verified. Due to these variations, many vertical soundings of the atmosphere would have to be obtained in order to characterize a mean atmosphere for the region of interest. Thunderstorm activity, multiple cloud-layers, and the spatial variation in the atmospheric structure have led to a hypothesis that deep-convection was responsible for the major differences between observed and predicted aerosol extinction profiles. If this is the case, a simple modification to the weak-convective model may be made to apply to a deep-convection model.

The results described above, clearly show that NOVAM is not yet ready to be used operationally in regions where convection is the dominant process. The following are recommendations for consideration in the improvement and development of NOVAM:

1. In order to eliminate the bias in wind speed measurements caused by avoiding areas of storm activity, wind measurements from buoys placed strategically in the area of operations would be invaluable in generating the 24 hour average winds.

2. Conduct experiments in the MARATHON area and other areas where weak convective conditions are expected. The data and results from these experiments could then be compared with the data and results from the KEY90 experiment.

3. Continue to explore the possibility that some cases that are currently classified as weak convection may in fact be examples of deep convection. If this hypothesis is correct, the parameters used to differentiate between shallow and deep convection need to be modified.

4. Explore the possibility of using satellite information to improve model predictions. One example would be to use the techniques established by Durkee, et al. (1986; 1990) to determine variations in optical depth (total extinction) over a horizontal path which could then be incorporated into NOVAM.

5. A comparison needs to be performed between what the current model is producing (LOWTRAN/NAM) against what NOVAM, incorporated in LOWTRAN, predicts (transmittance predictions versus measured would be extremely useful).

LIST OF REFERENCES

Albrecht, B. A., 1979: A Model of the Thermodynamic Structure of the Trade-Wind Boundary Layer.*J. Atmos. Sci., 36,* 73-98.

Augstein, E., 1976: Boundary Layer Observations Over the Oceans. In: European Centre for Medium Range Weather Forecasts, Seminars on the Treatment of the Boundary Layer in Numerical Weather Prediction ,pp. 138-182.

Davidson, K. L., and C. W. Fairall, 1986: Optical Properties of the Marine Atmospheric Boundary Layer: Aerosol Profiles. In: Proc. of SPIE,Vol. 637, Ocean Optics VIII , pp. 18-24.

_____, G. de Leeuw, S. G. Gathman, and D. Jensen, 1990: Verification of the Naval Oceanic Vertical Aerosol Model during FIRE. FIRE Science Results 1989, Monterey Ca., July 10-14, 1989, NASA Conference Publ. 3079, 6 pages.

de Leeuw, G., K. L. Davidson, 1988: Mixed-Layer Profiling with LIDAR and Modeling of the Aerosol Vertical Structure. NATO Advanced Workshop on Humidity Exchange over the Sea, De B.H./Epe, In: V.A. *Oost* , S.D. Smith and K.B. Ratseros (Eds.), The Netherlands, Apr. 25-29, 1988, pp. 100-104.

_____, _____, S. G. Gathman, and R. V. Noonkester, 1989: Physical Models for Aerosol in the Marine Mixed-layer. Proc. AGARD electromagnetic wave propagation panel specialists' meeting on "Operational decision aids for exploiting or mitigating electromagnetic propagation effects", San Diego Ca., May 15-19, 1989, pp. 40-1 to 40-8.

_____, _____, _____, and _____, 1989: Modeling of Aerosols in the Marine Mixed-layer. In: Proc. of SPIE, Vol. 1115, Propagation Engineering ,pp. 287-293.

_____, Ir. G. J. Kunz, and M. M. Moerman, 1991: Lidar and Aerosol Measurements by the TNO Physics and Electronics Laboratory During KEY90 (Marathon,

Florida, USA; July 2-19, 1990). TNO Physics and Electronics Laboratory, Report FEL-90-B375, 63 pages.

Durkee, P. A., D. R. Jensen, E. E. Hindman, and T. H. Vonder Haar, 1986: The relationship between marine aerosol particles and satellite-detected radiance, *J. Geophys. Res.*, ***91,*** 4063-4072.

_____, F. Pfeil, E. Frost, and R. Shema, 1990: Global analysis of aerosol particle characteristics, *Atmospheric Environment,* in press, 30 pages.

Fairall, C. W., and S. E. Larsen, 1983: Dry Deposition, Surface Production and Dynamics of Aerosols in the Marine Boundary Layer. *Atmospheric Environment, **18,*** 69-77.

_____, K. L. Davidson, and G. E. Schacher, 1983: Application of a Mixed-layer Model to Aerosols in the Marine Boundary Layer. *Tellus , **36B,*** 203-211.

_____, and _____, 1986: Dynamics and Modeling of Aerosols in the Marine Atmospheric Boundary Layer. In: E.C. Monahan and G. MacNiocaill (eds.): Oceanic Whitecaps and their Role in Air-sea Exchange Processes , Dordrecht, D. Reidel, pp. 195-208.

Fitzgerald, J. W., 1978: On the Growth of Aerosol Particles with Relative Humidity. *NRL Memorandum Report 3847,* Aug. 1978, 11 pages.

Gathman, S. G., 1978: Model for Estimating Meteorological Profiles from Shipboard Observations. Navy Research Laboratory, Washington D.C., NRL Report 8279.

_____, 1983: Optical Properties of the Marine Aerosol as Predicted by the Navy Aerosol Model. *Opt. Eng., **22,*** 57-62.

_____, 1984: Navy Hygroscopic Aerosol Model. In: L.H.Ruhnke and A.Deepak (eds.): Hygroscopic Aerosols , A. Deepak Publ., pp. 93-115.

_____, 1989: A Preliminary Description of NOVAM, the Navy Oceanic Vertical Aerosol Model. Navy Research Laboratory, Washington D.C., *NRL Report 9200*, June 1989, 22 pages.

_____, G. de Leeuw, K. L. Davidson, and D. R. Jensen, 1989: The Naval Oceanic Vertical Aerosol Model: Progress Report. Proc. AGARD meeting on "Atmospheric propagation in the UV, visible,IR and mm-wave region and related system aspects", 11 pages.

_____, 1991: personal communication.

Gerber, H. E., 1985: Relative Humidity Parameterization of the Navy Aerosol Model (NAM). Navy Research Laboratory, Washington D.C., *NRL Report 8956*, Dec. 1989, 13 pages.

Griggs, M., 1985: A Method to Correct Satellite Measurements of Sea Surface Temperature for the Effect of Atmospheric Aerosols. *J. Geophys. Res.*, **90**, 12951-12959.

Hooper, W. ,1991: personal communication.

Hoppel, W. A., J. W. Fitzgerald, G. M. Frick, R. E. Larson, and E. J. Mack, 1989: Atmospheric Aerosol Size Distributions and Optical Properties Found in the Marine Boundary Layer Over the Atlantic Ocean. *NRL Report 9188*,pp. 36,45-53.

Hudson, R. D., 1969: Infrared system Engineering , J. Wiley and Sons Publ., page 115.

Hughes, H. G., 1987: An Evaluation of the LOWTRAN 6 Navy Maritime Aerosol Model Using 8 to 12 μm Sky Radiances. *Opt. Eng.* , **26**, 1155-1160.

Jensen, D. R., 1990: Evaluation of the Navy Oceanic Vertical Aerosol Model Using Lidar and PMS Particle-size Spectrometer. Naval Ocean Systems Center, San Diego Ca., *NOSC TR 1391*, Dec. 1990, 18 pages.

Kneizys, F. X., E. P. Shettle, L. W. Abreu, J. H. Chetwynd, G. P. Anderson, W. O. Gallery, J. E. A. Shelby, and S. A. Clough, 1988: User's Guide to LOWTRAN 7. Air Force Geophysics Laboratory, Hanscom AFB Mass., AFGL-TR-88-0177, Aug. 1988, 146 pages.

Monahan, E. C., K. L. Davidson, and D. E. Spiel, 1982: Whitecap Aerosol Productivity Deduced from Simulation Tank Measurements. *J. Geophys. Res.*, 87, 8898-8904.

_____, C. W. Fairall, K. L. Davidson, and , P. J. Boyle, 1983: Observed Inter-relations Between 10m Winds, Ocean Whitecaps and Marine Aerosols. *Quart. J. Roy. Met. Soc., 109,* 379-392.

Noonkester, V. R., 1981: Aerosol and Humidity Structure Beneath Maritime Stratus Clouds: A Review of Theory, Models, and Observations. Naval Ocean Systems Center, San Diego Ca., *NOSC TN 1070*, Oct. 1981, 61 pages.

_____, 1985: Profiles of Optical Extinction Coefficients Calculated from Droplet Spectra Observed in Marine Stratus Cloud Layers. *J. Atmos. Sci., 42,* 1161-1171.

_____, 1986: Model of IR Extinction by Aerosols Beneath Marine Stratus Clouds; A Computer Program for the Navy Oceanic Vertical Aerosol Model (Category A). Naval Ocean Systems Center, San Diego Ca., *NOSC TD 966* , Sept. 1986.

ONTAR Corporation, 1990: Manual for the Personal Computer Version of the AFGL LOWTRAN7 Atmospheric Model (PCTRAN.7) ; Version 2. 332 pages.

Rao, P. K., S. J. Holmes, R. K. Anderson, J. S. Winston, P. E. Lehr, eds. 1990: Weather Satellites: Systems, Data, and Environmental Applications. *American Meteorological Society*,pp. 408,413-415.

INITIAL DISTRIBUTION LIST

		No. Copies
1.	Defense Technical Information Center Cameron Station Alexandria, VA 22304-6145	2
2.	Library, Code 52 Naval Postgraduate School Monterey, CA 93943-5002	2
3.	Chairman (Code OC/Co) Department of Oceanography Naval Postgraduate School Monterey, CA 93943-5000	1
4.	Chairman (Code MR/Hy) Department of Meteorology Naval Postgraduate School Monterey, CA 93943-5000	1
5.	Professor K. L. Davidson (Code MR/Ds) Department of Meteorology Naval Postgraduate School Monterey, CA 93943-5000	1
6.	Professor P. A. Durkee (Code MR/De) Department of Meteorology Naval Postgraduate School Monterey, CA 93943-5000	1
7.	Dr. M. Rouault (Code MR/Rt) Department of Meteorology Naval Postgraduate School Monterey, CA 93943-5000	1
8.	LT T. H. Cecere, USN 146 Avenue A Holbrook, NY 11741	1
9.	Dr. J. Richter (Code 54) Naval Ocean Systems Center 271 Catalina Blvd. San Diego, CA 92152	1
10.	S. Gathman (Code 543) Naval Ocean Systems Center 271 Catalina Blvd. San Diego, CA 92152	1

11. Dr. G. de Leeuw 1
TNO Physics and Electronics Laboratory
Oude Waalsdorperweg 63
P.O. Box 96864
2509 JG The Hague
The Netherlands

12. Dr. M. H. Smith 1
Physics Dept.
UMIST
P.O. Box 88
Manchester M601QD, UK

13. Dr. B. Hooper (Code 4112) 1
Naval Research Laboratory
Washington, D.C. 20375

Thesis
C3383445 Cecere
c.1 An evaluation of the Naval Oceanic Vertical Aerosol Model during Key90.